AD-A061 791 NAVAL SURFACE WEAPONS CENTER DAHLGREN LAB VA F/G 20/4
OGIVE CYLINDER MODIFIED FOR NEAR MINIMUM SIDE MOMENT.(U)
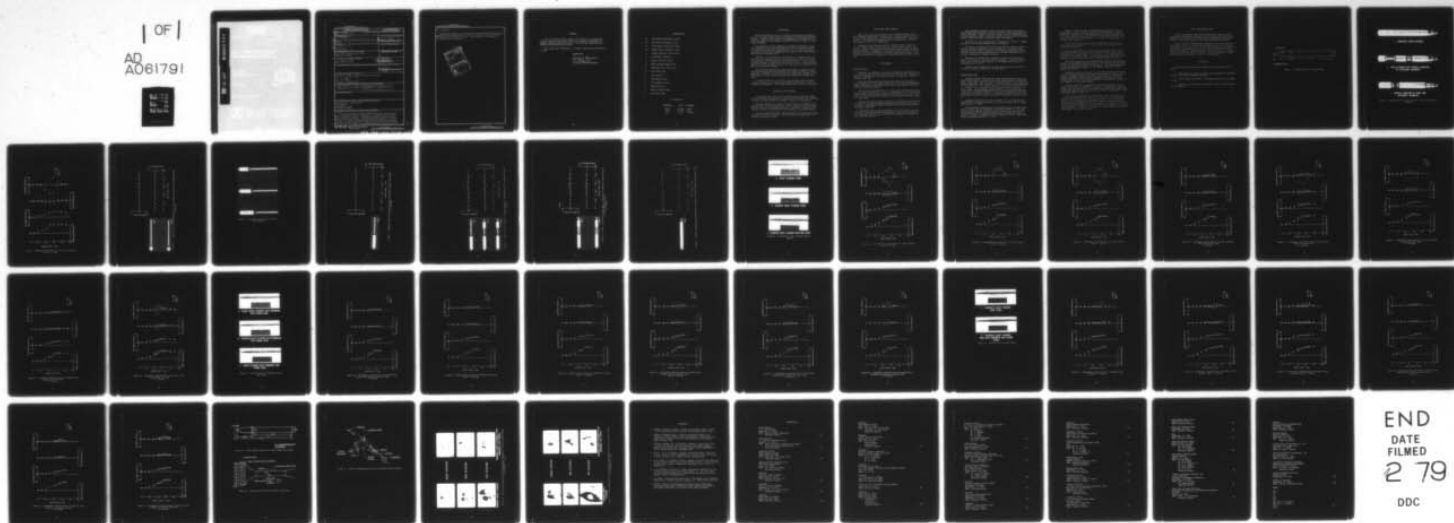OCT 78 P DANIELS
UNCLASSIFIED NSWC/DL-TR-3873 NL

1 OF 1
AD
A061791

END
DATE
FILMED
2 79
DDC

REPORT DOCUMENTATION PAGE		READ INSTRUCTIONS BEFORE COMPLETING FORM
1. REPORT NUMBER NSWC/DL-TR-3873	2. GOVT ACCESSION NO.	3. RECIPIENT'S CATALOG NUMBER
4. TITLE (and Subtitle) OGIVE CYLINDER MODIFIED FOR NEAR MINIMUM SIDE MOMENT		5. TYPE OF REPORT & PERIOD COVERED Final Rept. 6. PERFORMING ORG. REPORT NUMBER
7. AUTHOR(s) PETER DANIELS		8. CONTRACT OR GRANT NUMBER(s)
9. PERFORMING ORGANIZATION NAME AND ADDRESS Naval Surface Weapons Center (K20) Dahlgren, VA 22448		10. PROGRAM ELEMENT, PROJECT, TASK AREA & WORK UNIT NUMBERS NIF
11. CONTROLLING OFFICE NAME AND ADDRESS Naval Weapons Center China Lake, CA 93557		12. REPORT DATE October 1978 13. NUMBER OF PAGES 55
14. MONITORING AGENCY NAME & ADDRESS(if different from Controlling Office)		15. SECURITY CLASS. (of this report) UNCLASSIFIED 15a. DECLASSIFICATION/DOWNGRADING SCHEDULE

16. DISTRIBUTION STATEMENT (of this Report)

Approved for public release; distribution unlimited.

54 p.

17. DISTRIBUTION STATEMENT (of the abstract entered in Block 20, if different from Report)

F32301   WF32301000

18. SUPPLEMENTARY NOTES

19. KEY WORDS (Continue on reverse side if necessary and identify by block number)

composite ogive cylinder model
side moments
asymmetric vortices
conventional models

20. ABSTRACT (Continue on reverse side if necessary and identify by block number)

Bodies of revolution develop side moments at large angles of attack due to asymmetric vortices. Consequently, a composite ogive cylinder model was designed in order to determine what modifications were necessary to suppress this moment. Low speed wind tunnel tests, in which the geometry of the model was systematically varied, revealed that a simple afterbody step down coupled with slight nose bluntness could reduce side moment by over 90% compared to the unmodified model. (Continued on back.)

(20. Continued)

Conventional models were constructed in order to substantiate the results obtained with the composite model. Tests were conducted at three different velocities (85 mph, 120 mph, 140 mph). Large reduction in side moments (90% reductions) were obtained.

ACCESSION for

NTIS	White Section
DDC	Buff Section
UNANNOUNCED	
JUSTIFICATION	

BY

DISTRIBUTION/AVAILABILITY CODES

Di.		SPECIAL
A		
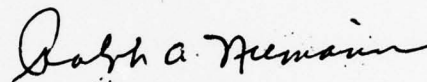
FOREWORD

The work reported herein presents the results of an experimental research program to determine a method for minimizing side moment on a symmetric pointed body of revolution. This work was authorized under AIRTASK A03W-350D/004B/7F32-301-000.

This report was reviewed by H. P. Caster, head, Exterior Ballistics Division.

Released by:

R. A. NIEMANN, Head
Strategic Systems Department

iii

NOMENCLATURE

C_n Side moment coefficient, n/Qsd

C_Y Side force coefficient, Y/Qs

C_m Pitch moment coefficient, M/Qsd

C_N Normal force coefficient, N/Qs

Q Dynamic pressure, $\frac{1}{2}\rho V^2$ (lb/ft^2)

ρ Air density (slug/ft^3)

V Tunnel velocity (ft/sec)

d Model maximum diameter (ft)

S Reference area, $\pi d^2/4$ (ft^2)

r_n Nose radius (ft)

Y Side force, lb

n Side moment, ft/lb

M Pitch moment, ft/lb

N Normal force, lb

α Angle of attack (deg)

ϕ Roll angle (deg)

SI CONVERSION

Multiply	By	To Obtain
degree	0.01745	radian
foot	0.3048	meter
pound	0.4536	kilogram

iv

INTRODUCTION

Efficient high-speed flight of missiles and aircraft necessitates the use of slender pointed fuselage forebodies for aerodynamic drag minimization. However, these slender pointed bodies develop significantly large side moments at high angles of attack[1-4] that can result in flight control problems.

The alleviation of this problem is of particular interest to aircraft designers since these side moments can have a predominant effect on aircraft stall and spin characteristics. It is also of interest to the missile designer who contemplates the design of highly maneuverable guided missile configurations.[5]

Generally, it is agreed that side moments on a symmetric body are the result of asymmetric vortices that develop at high angles of attack. The phenomenon is complicated by a switching effect; i.e., side forces have been observed to change direction with roll angle. Side forces and moments are relatively more severe at low velocities and gradually diminish as the velocity increases.

Jorgensen[6] has measured side forces and moments on numerous configurations and showed that body geometry has a strong influence on their magnitude. Therefore, it was felt that given sufficient freedom to vary body geometry, shapes could be evolved that develop near minimum side moment.

A composite model of a 10-caliber ogive cylinder, whose schematic is shown in Figure 1, was fabricated and wind tunnel tested in order to evaluate this hypothesis. This paper presents the results of that study.

COMPOSITE OGIVE CYLINDER

A composite model (CPM) of a 10-caliber ogive cylinder was fabricated at the Naval Surface Weapons Center, White Oak Laboratory (NSWC/WO), in order to study the effect of geometry variation on side moment.

The basic configuration shown in Figure 2a has its component parts supported by a steel rod through the center. The parts may be disassembled by unscrewing the threaded nose cap. The base of the model is designed to contain a sting mounted, four component, strain gage balance.

Figure 2 compares the basic configuration with configurations having radical variations in geometry. These variations are shown only to illustrate the models' utility.

1

WIND TUNNEL TEST PROCEDURE

Static force tests were conducted in the Edgewood Arsenal 28- by 40-in. subsonic wind tunnel.[7] Normal force, pitching moment, side force, and side moment coefficients were measured in aeroballistic axes (non-rolling). All moments are referenced about the model base. Angles of attack from 0 to 90° were investigated.

Preliminary tests revealed that the composite model, because of a lack of rigidity, could only be tested at tunnel velocities less than 100 mph. Model vibrations above this velocity were too severe to obtain good quality data. Consequently, initial tests were conducted at 85 mph because of the good performance of the model and balance system. Later tests were conducted on conventionally fabricated models at higher velocity.

TEST RESULTS

COMPOSITE MODEL

Initially, the variation of the static stability coefficients with angle of attack and for roll angles of 0, 90, and 180° were evaluated for the basic configuration (ogive cylinder shown in Figure 2a). Figure 3 presents these data.

The side moment coefficient changes sign with roll angle as expected[4] and has a maximum value nearly equal to half the pitching moment. Slight differences in the normal force and pitching moment coefficients with roll angle were obtained.

The initial runs showed that it was very time consuming to properly roll the composite model on its sting. Consequently, it was decided that further tests on the composite model would be conducted at a roll angle of 0° and the pertinent test results be verified with conventional models at a later date.

Figure 4 presents the lateral stability characteristics versus angle of attack for the minimum volume configuration with pointed and blunted nose caps. The lateral stability coefficients for these configurations are small as expected.

The blunted nose cap was introduced at this time since it had been shown that nose blunting reduces side moment.[6] The thickened rear section (cylinder-cone frustum) of the model is required as a housing for the strain gage balance.

The cylinder-cone frustum (that is the rear portion of the model) was systematically extended, as shown in Figure 5, until appreciable side moments developed. Figure 6 shows the lateral stability characteristics and near maximum cylinder-cone frustum length for near minimum side moment. Longer lengths were shown to generate large side moments.

The effect of nose reconstruction is presented in Figure 7. Further lengthening of the nose generated large side moments.

The effect of reducing the resulting gap depth is shown in Figure 8. Further gap depth minimization was not attempted. The blunted ogive cylinder with gap, shown in Figure 8, has a maximum side moment of less than 10% of the side moment developed by its pointed counterpart with straight afterbody (see Figures 2a and 3).

Restoring the afterbody to a constant cross section, as shown in Figure 9, resulted in large side forces and moments. Comparing Figure 3 with Figure 9 indicates no reduction in side moment due to the nose bluntness ($r_n/d = 0.1725$).

Further testing showed that the step down (behind the nose) had to be abrupt in order to produce the desired effect.

CONVENTIONAL MODEL

Convention models (CVM) made up of nose and afterbody sections were fabricated in order to evaluate test results obtained with the composite model. These models were also used to study the effect of roll angle and velocity variation. Roll angles of 0, 90, 180, and 270° were investigated at velocities of 85, 120, and 140 mph which is the tunnel maximum velocity. Figure 10a is a photograph of the ogive cylinder test configuration (CVM). The aerodynamic characteristics of this configuration at 85 mph are in excellent agreement with the results obtained for its CPM counterpart (see Figures 3 and 11). Aerodynamic characteristics for the ogive cylinder (CVM) at higher velocities are presented in Figures 12 and 13.

Comparing Figures 11 and 13 with Figures 12, it is noted that the primary effect of changing velocity is to cause the side force to change direction at $\phi = 90,270°$.

The aerodynamic characteristics of the blunted ogive cylinder (CVM), shown in Figure 10b, are presented in Figures 14 through 16. The side forces and side moments are significantly reduced at 85 mph and are in poor agreement with the composite blunted ogive cylinder data shown in Figure 9. However, at higher velocities (Figures 15 and 16), large side forces and moments develop at $\phi = 270°$.

3

Figures 17 and 18 present the aerodynamic characteristics of the blunted ogive cylinder with gap (CVM), whose configuration is shown in Figure 10c. The data is in good agreement with the composite model at V = 85 mph, and side forces and moments are considerably reduced. However, as the velocity is increased to V = 120 mph, the gap becomes considerably less effective.

It was felt that the step up (cone frustum) might be the cause of the increased side moments at V = 120 mph, and consequently the cone frustum was eliminated.

The two configurations in Figure 19 having blunted noses and two different afterbody step downs were fabricated and wind tunnel tested. One body had a step down equal to the step down of the composite model in Figure 8 (see square symbol). The step down of the other model (minimum step) was half of the depth of the composite model in Figure 8.

Both bodies experienced very minimal side moments at all velocities tested. The aerodynamic characteristics of the blunted ogive with minimum step is presented in Figures 20 through 22. No further minimization of the step down was attempted. An even smaller step down might be equally as effective.

Combining a pointed ogive with the step down afterbody (Figure 19c) did not sufficiently reduce the side forces and moments. This result is shown by comparing Figures 23 through 25 with Figures 20 through 22. Further improvement of the lateral aerodynamic characteristic of the pointed ogive with step down might have been accomplished by optimizing its geometry via the composite model.

Coe[4] has shown that a parabolic nose (without afterbody) does not exhibit side forces and moments at low speed. Consequently, a three-caliber nose was fabricated to be used with the seven-caliber afterbodies to provide comparison data with the ogive cylinder configurations. These models are shown in Figure 26.

Test results (Figures 27 through 29) showed that the parabolic nose cylinder body developed side forces and side moment that are somewhat smaller than the pointed or blunted ogive cylinder. The lateral characteristics of the parabolic nose cylinder with step down are further improved by the afterbody step down (see Figures 30 through 32). However, the blunt ogive cylinder with step down developed the lowest side forces and side moments. A schematic of the ogive cylinder modified for minimum side moment is presented in Figure 33.

4

FLOW VISUALIZATION STUDY

A flow visualization study of the leeward wake structure of the pointed ogive cylinder and the blunted ogive cylinder with step down was conducted in the University of Notre Dame low turbulence smoke tunnel. Figures 34 and 35 are sketches of the wind tunnel and test setup.[8]

Figures 36 and 37 compare smoke photographs of the ogive cylinders at angles of attack of 35 and 45° and a tunnel velocity of 30 ft/sec. Photographs of the pointed ogive cylinder show very distinct vortex cores, and it would appear that the presence of the blunt nose and step down diffuses the wake and somewhat diminishes the vortex strength. However, these conclusions are mainly conjecture. Flow visualization at higher angles of attack and higher velocity was unsatisfactory.

CONCLUSIONS

The following conclusions were made based on the results of this study.

1. Side moment on an ogive cylinder can be minimized at low speed by nose blunting and afterbody step down.

2. Proper design can result in side moment reduction on the order of 90%.

3. High-speed tests should be conducted in order to further evaluate the design.

TANGENT OGIVE

1.0

3.0

7.0
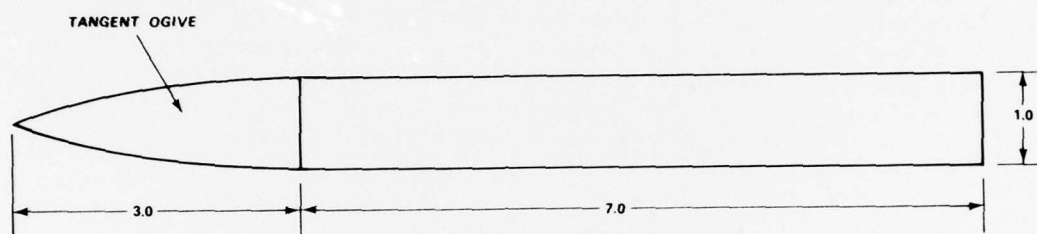
(ALL DIMENSIONS IN CALIBERS)

Figure 1. Schematic of Ogive Cylinder Model
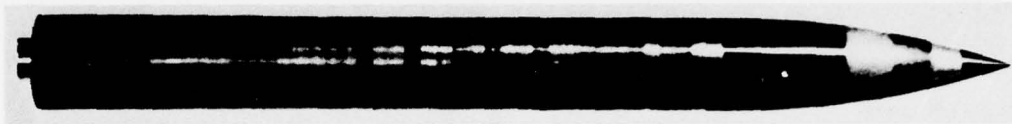
a. **COMPOSITE OGIVE-CYLINDER**
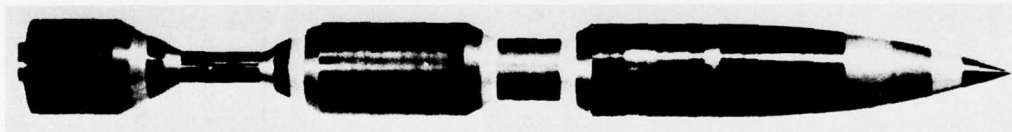
b. **OGIVE-CYLINDER WITH RADICAL VARIATION
OF AFTERBODY GEOMETRY**
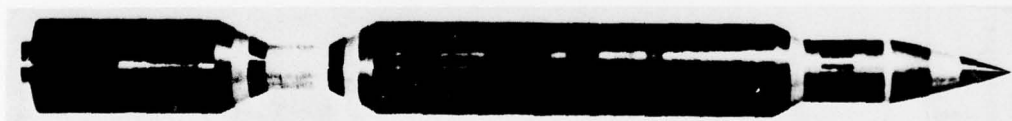
c. **RADICAL VARIATION OF NOSE AND
AFTERBODY GEOMETRY**

Figure 2.   Composite Model Showing Possible Radical Variations in
Geometry
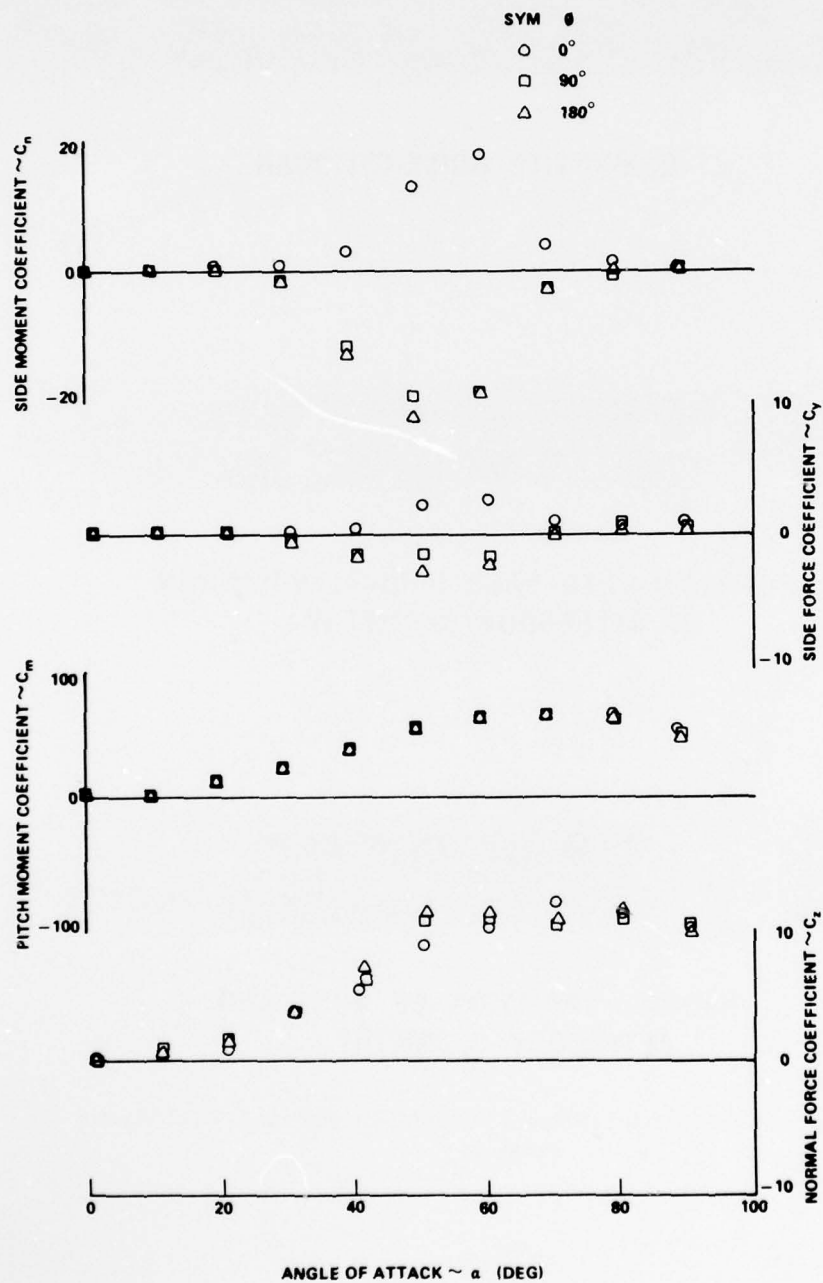
Figure 3. Aerodynamic Characterisitics of Ogive Cylinder
(CPM) V = 85 mph

8
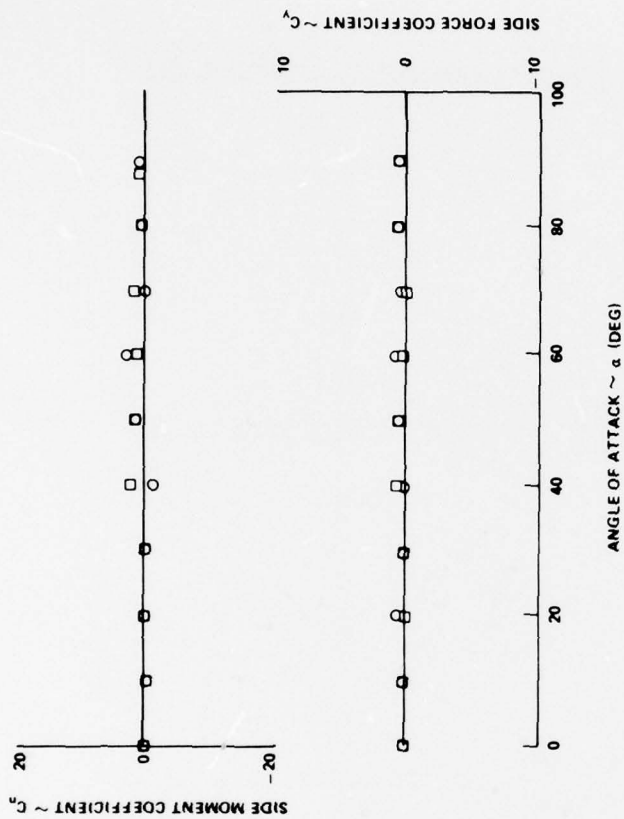
Figure 4. Lateral Stability Characteristics of the Composite Model with Minimum Volume
V = 85 mph
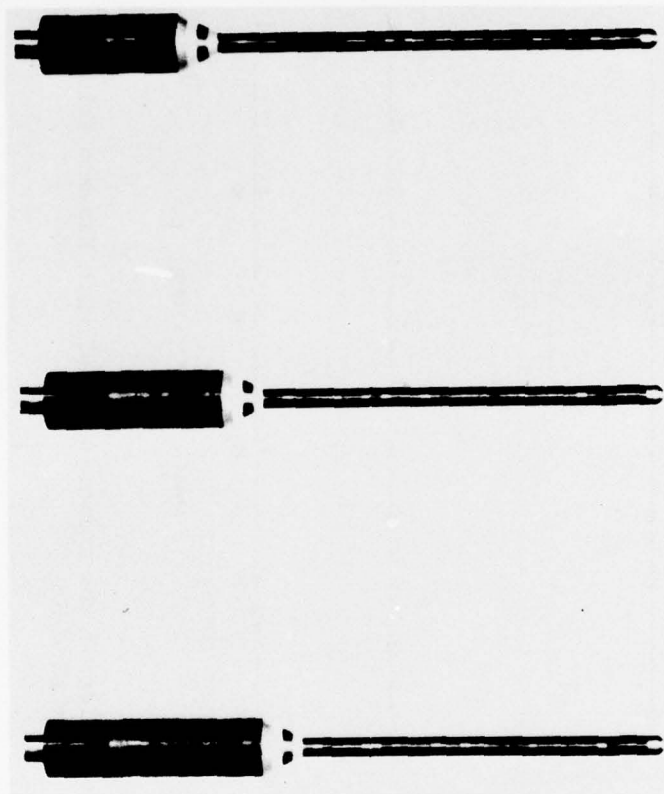
Figure 5.   Systematic Extension of Cylinder-
            Cone Frustum
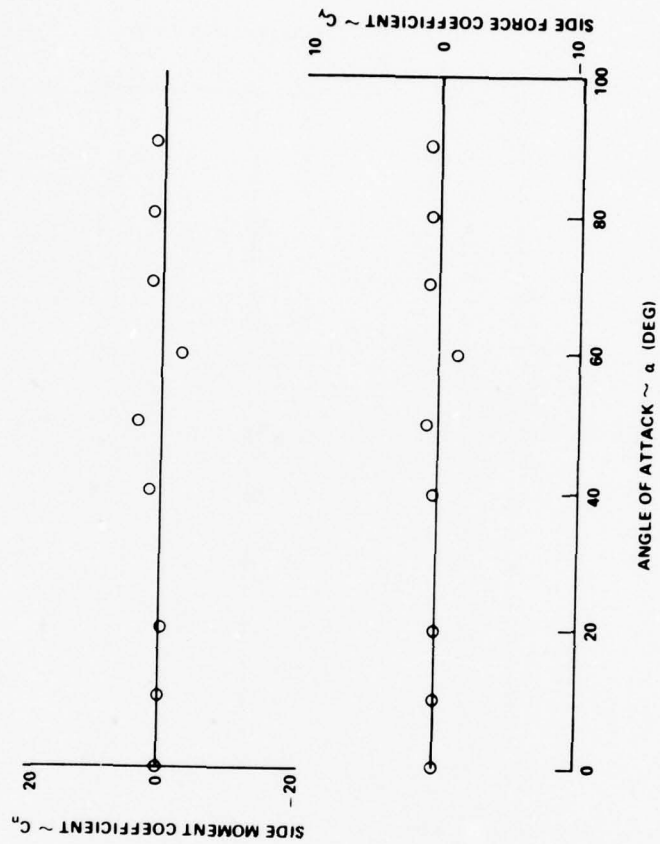
Figure 6. Maximum Length Cylinder-Cone Frustum for Near Minimum Side Moment
V = 85 mph

11
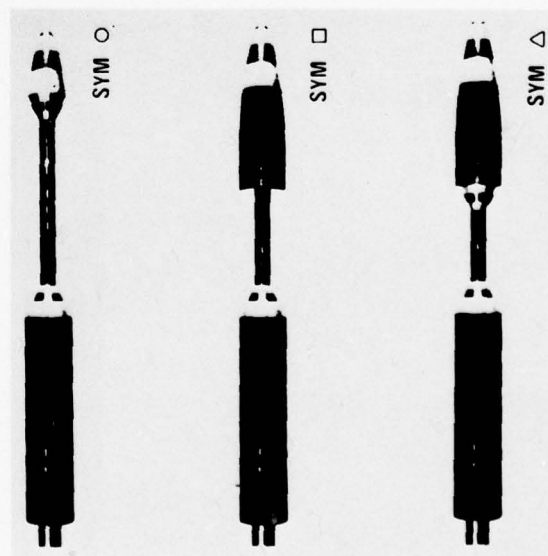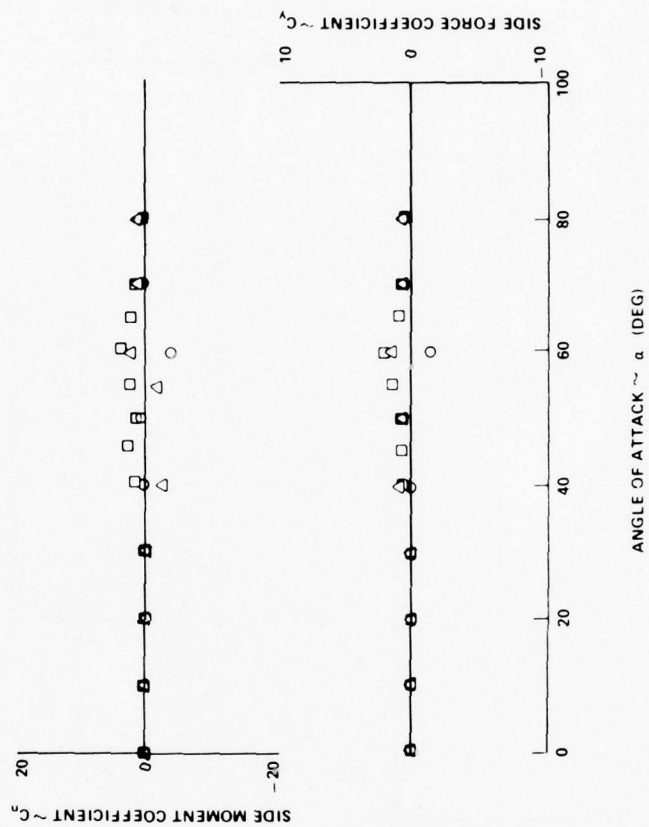
Figure 7. Effect of Nose Length on Lateral Stability Characteristics of Composite Model
V = 85 mph
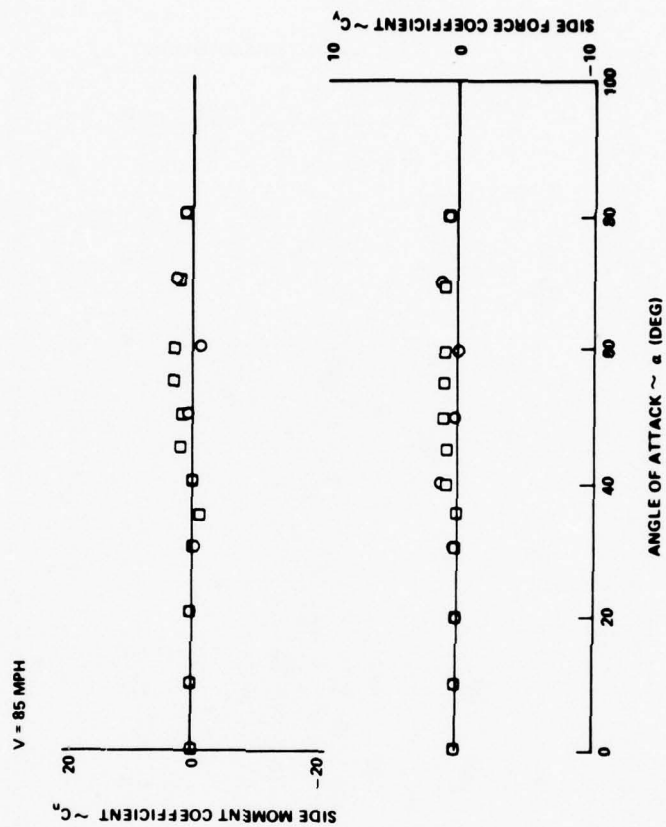
Figure 8. Effect of Minimizing Gap Depth on the Lateral Stability Characteristics
of the Composite Model
V = 85 mph

SIDE FORCE COEFFICIENT ~ C_Y

CN

SIDE FORCE COEFFICIENT ~ C_Y

ANGLE OF ATTACK ~ α (DEG)

SIDE MOMENT COEFFICIENT ~ C_n

SYM O
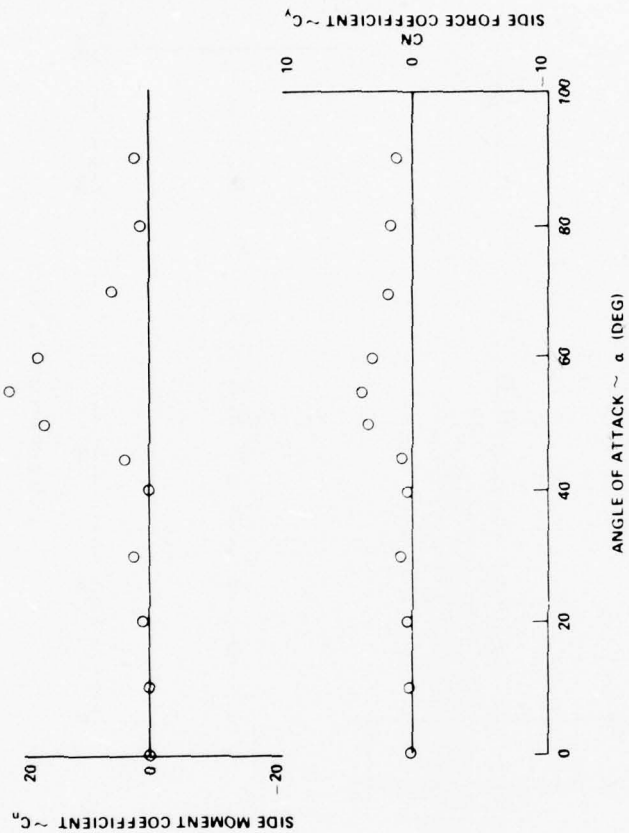
Figure 9. Lateral Stability Characteristics of Composite Ogive Cylinder with Blunted Nose
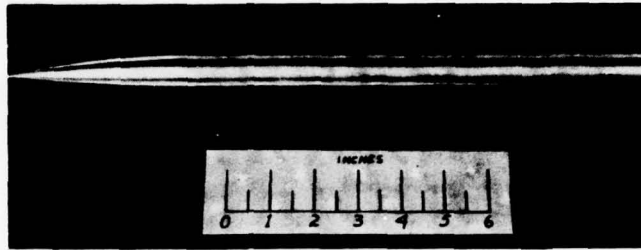
a. OGIVE CYLINDER (CVM)
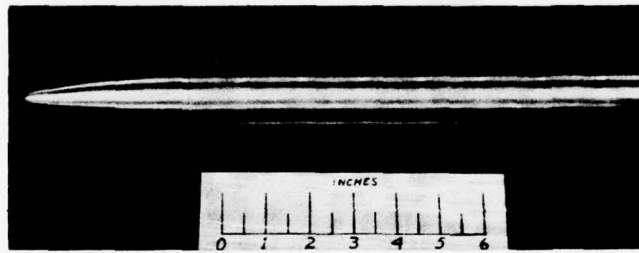
b. BLUNTED OGIVE CYLINDER (CVM)
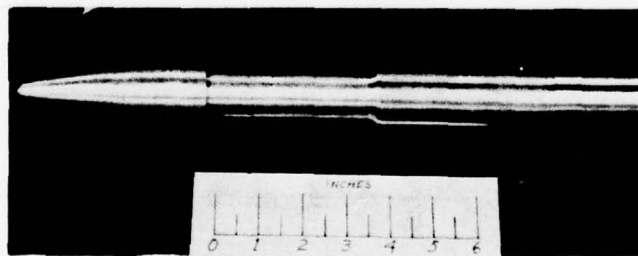
c. BLUNTED OGIVE CYLINDER WITH GAP (CVM)

Figure 10.   Conventional Ogive Cylinder Configu-
rations
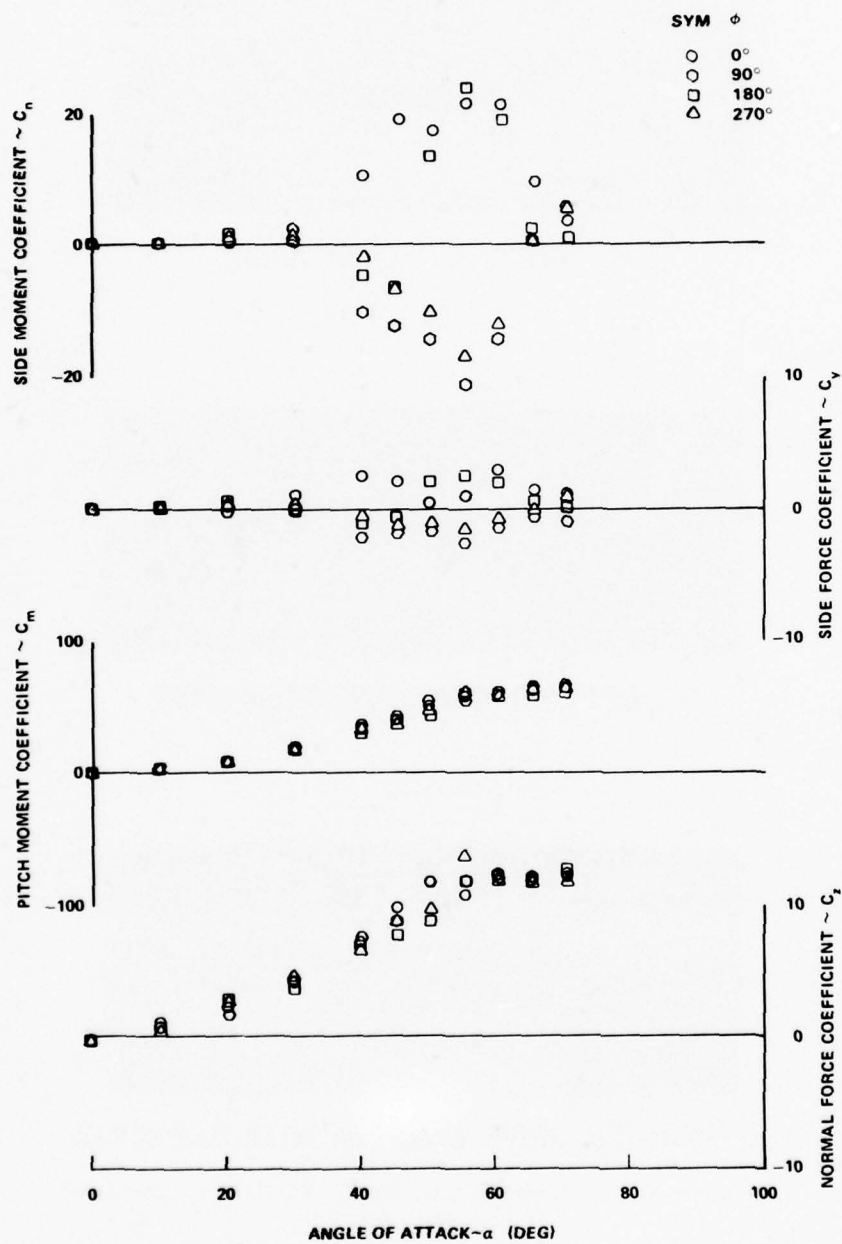
Figure 11. Aerodynamic Characteristics of Ogive Cylinder
(CVM) V = 85 mph

16
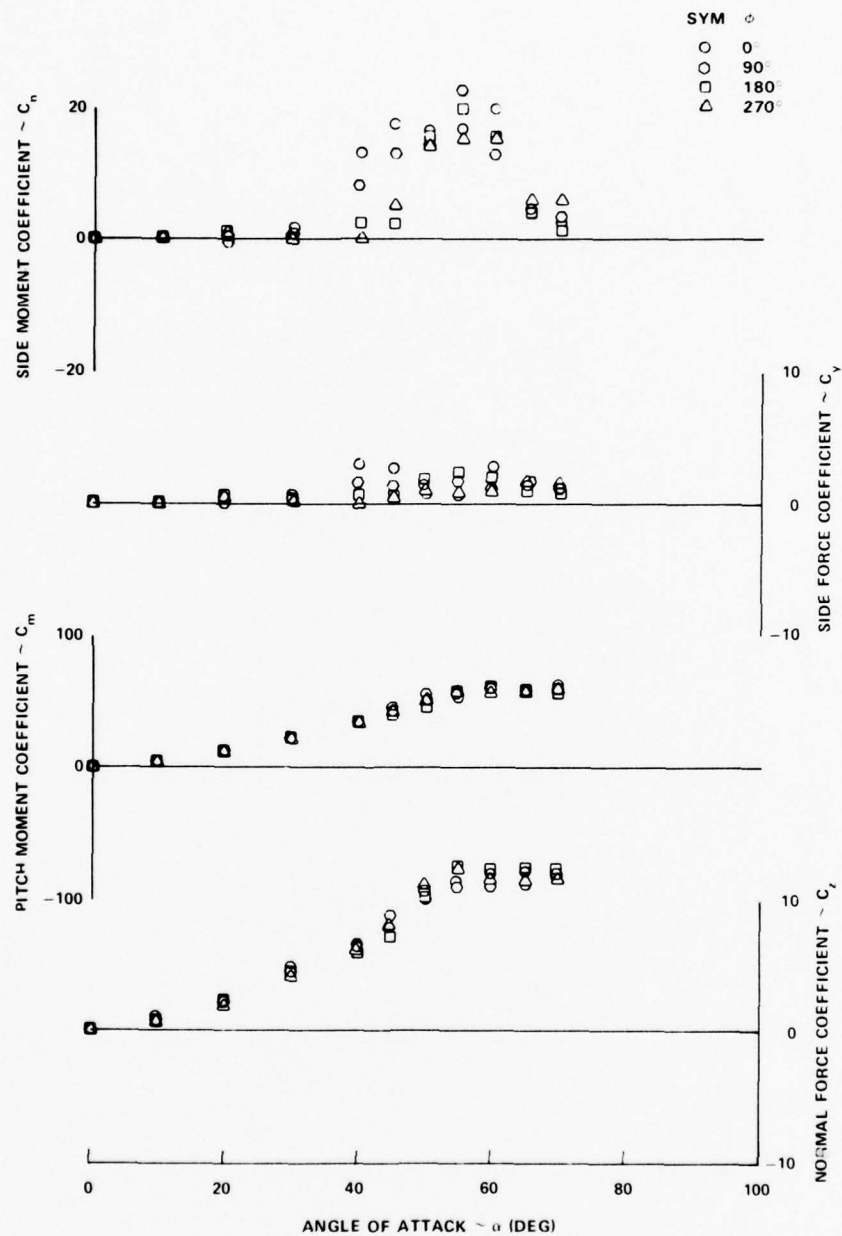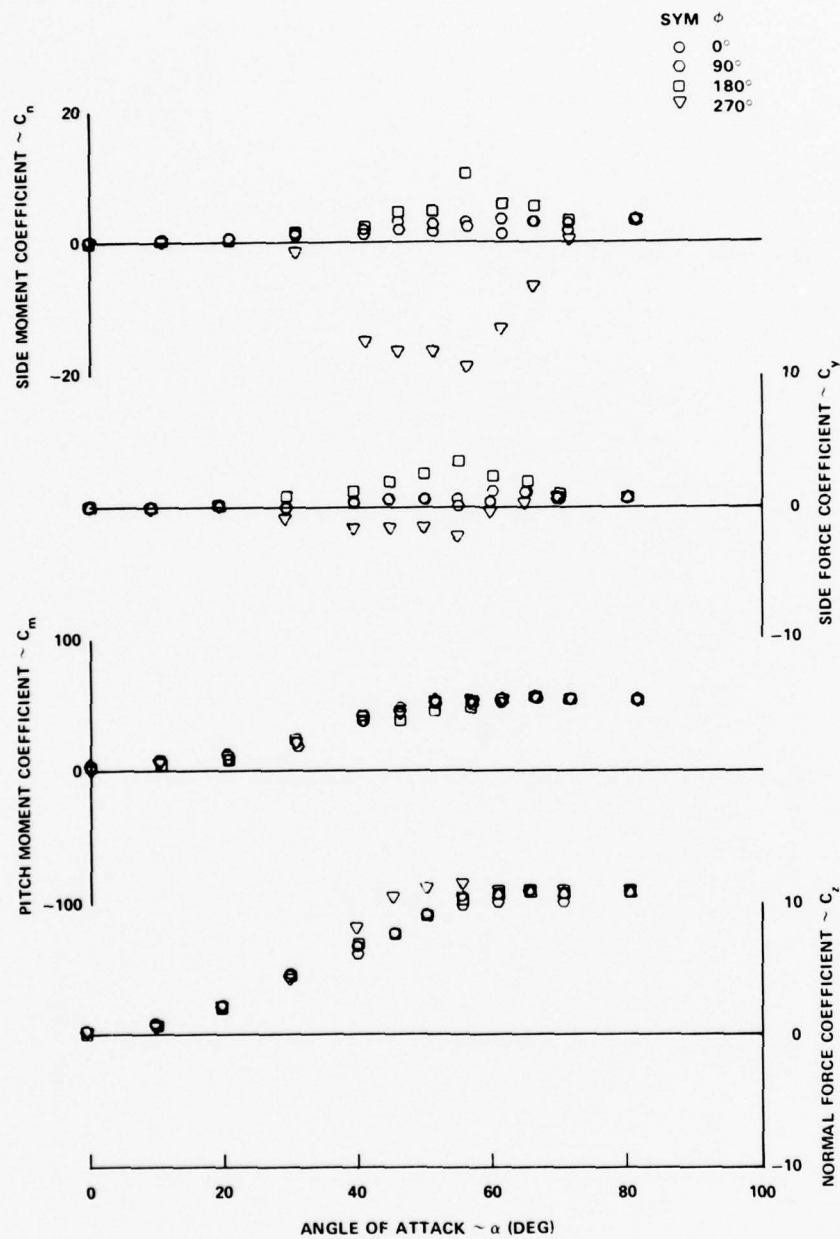
Figure 12.   Aerodynamic Characteristics of Ogive Cylinder
(CVM) V = 120 mph

17
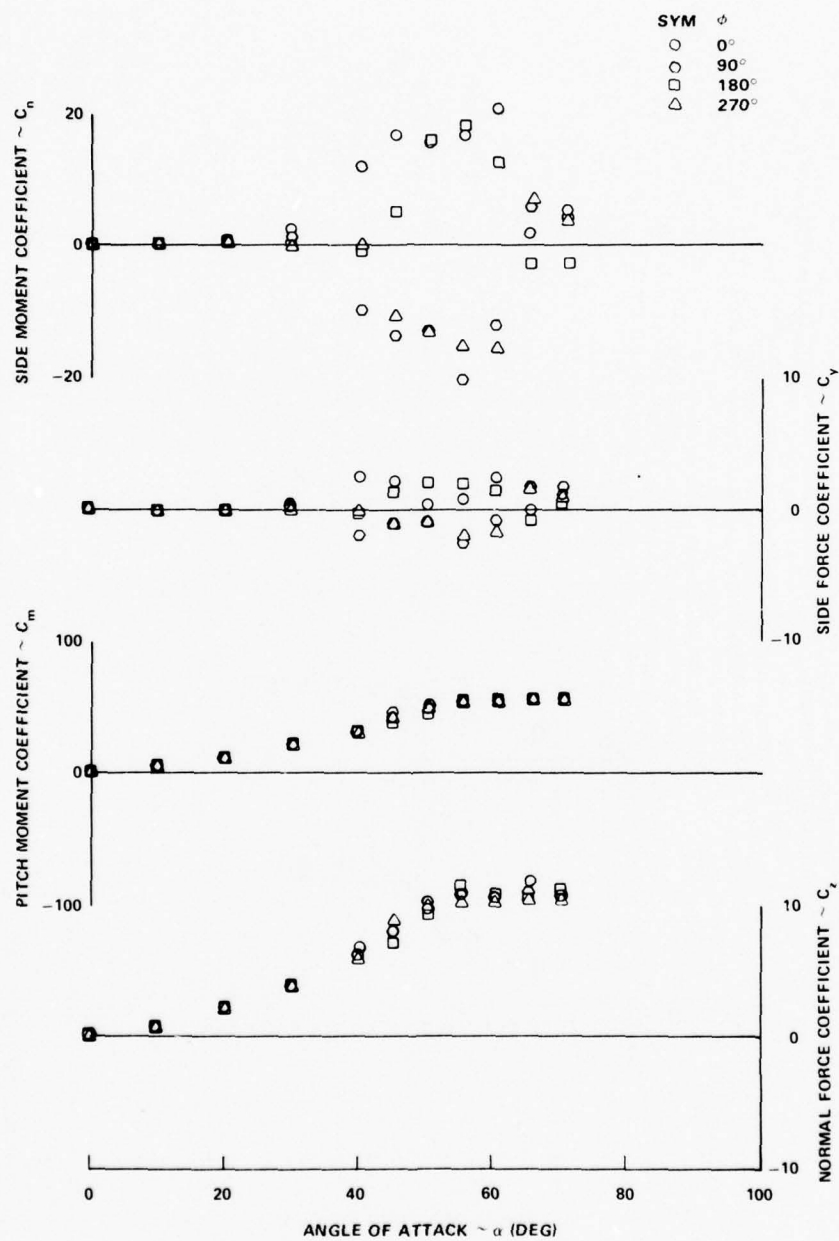
Figure 13. Aerodynamic Characteristics of Ogive Cylinder
(CVM) V = 140 mph

18
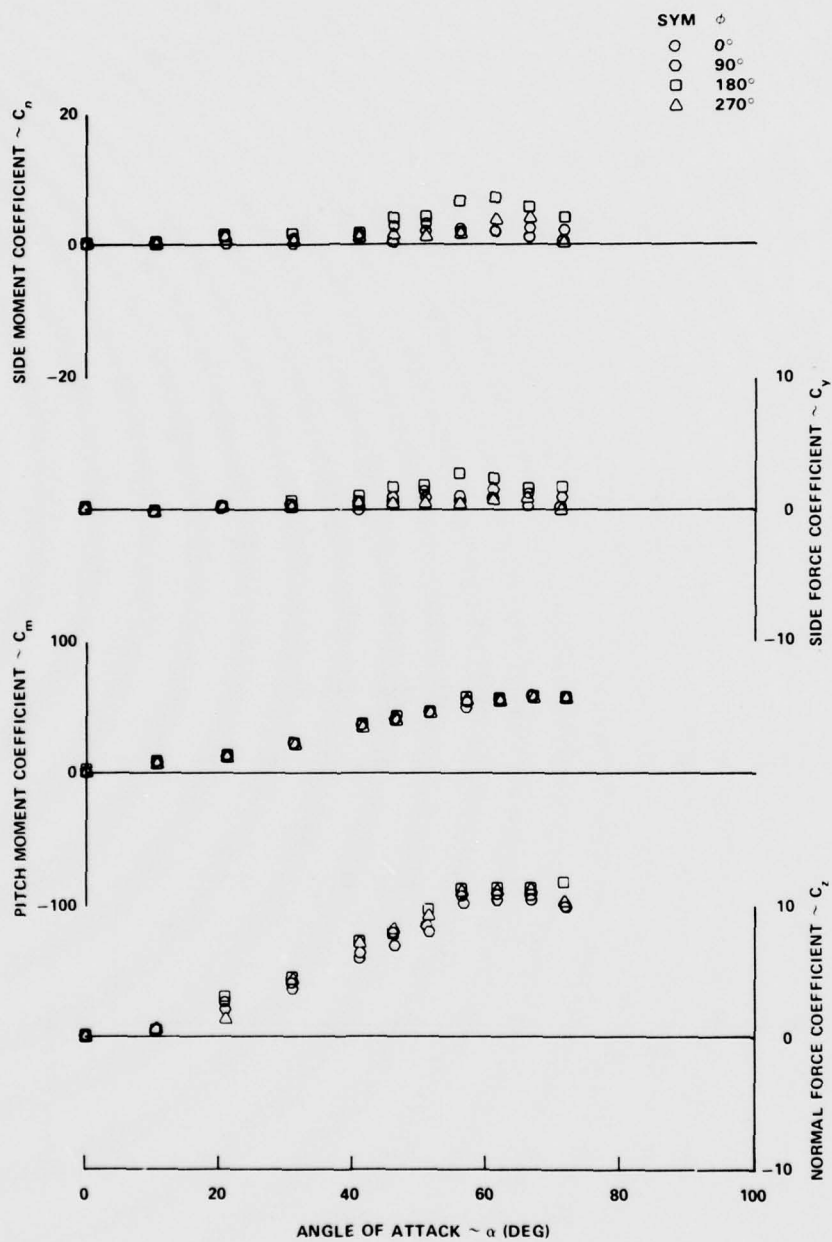
Figure 14. Aerodynamic Characteristics of Ogive Cylinder
with Blunted Nose (CVM)
V = 85 mph

19

Figure 15. Aerodynamic Characteristics of Ogive Cylinder
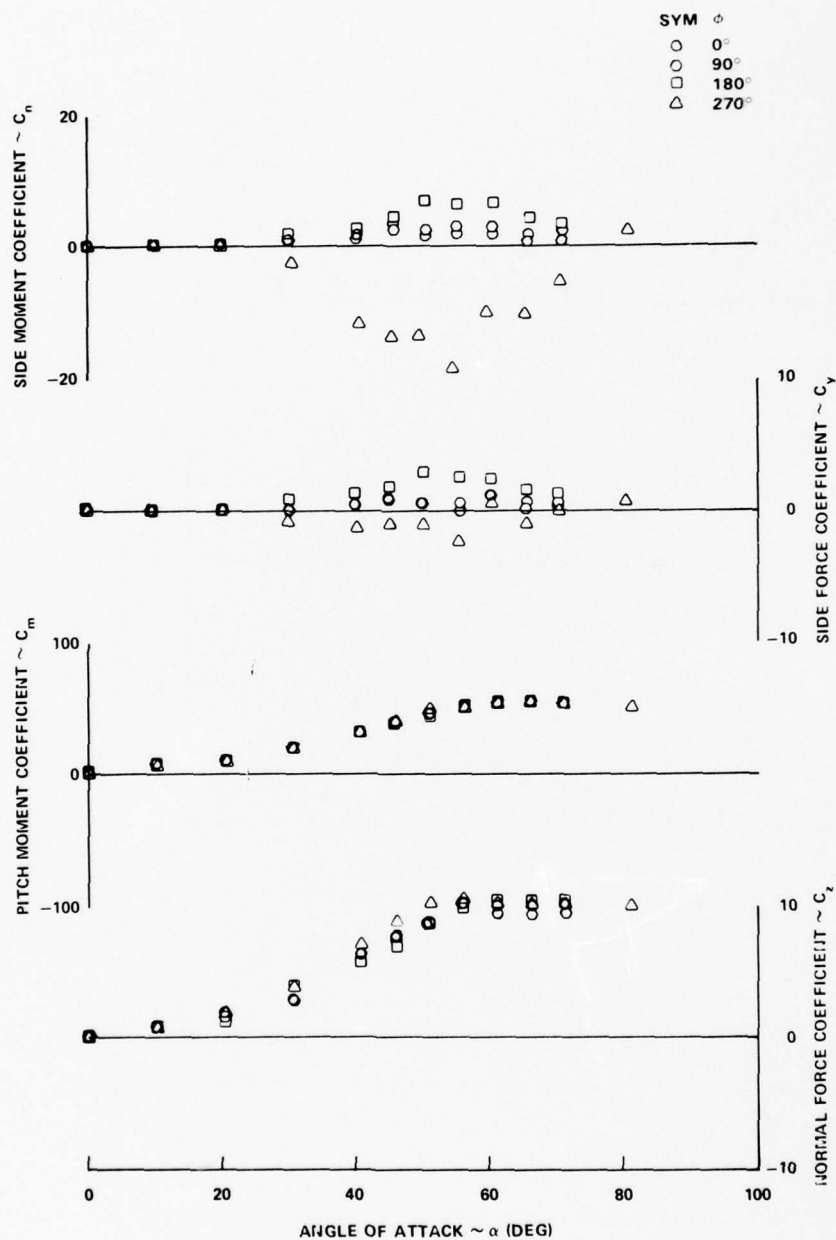with Blunted Nose (CVM)
V = 120 mph

Figure 16. Aerodynamic Characteristics of Ogive Cylinder
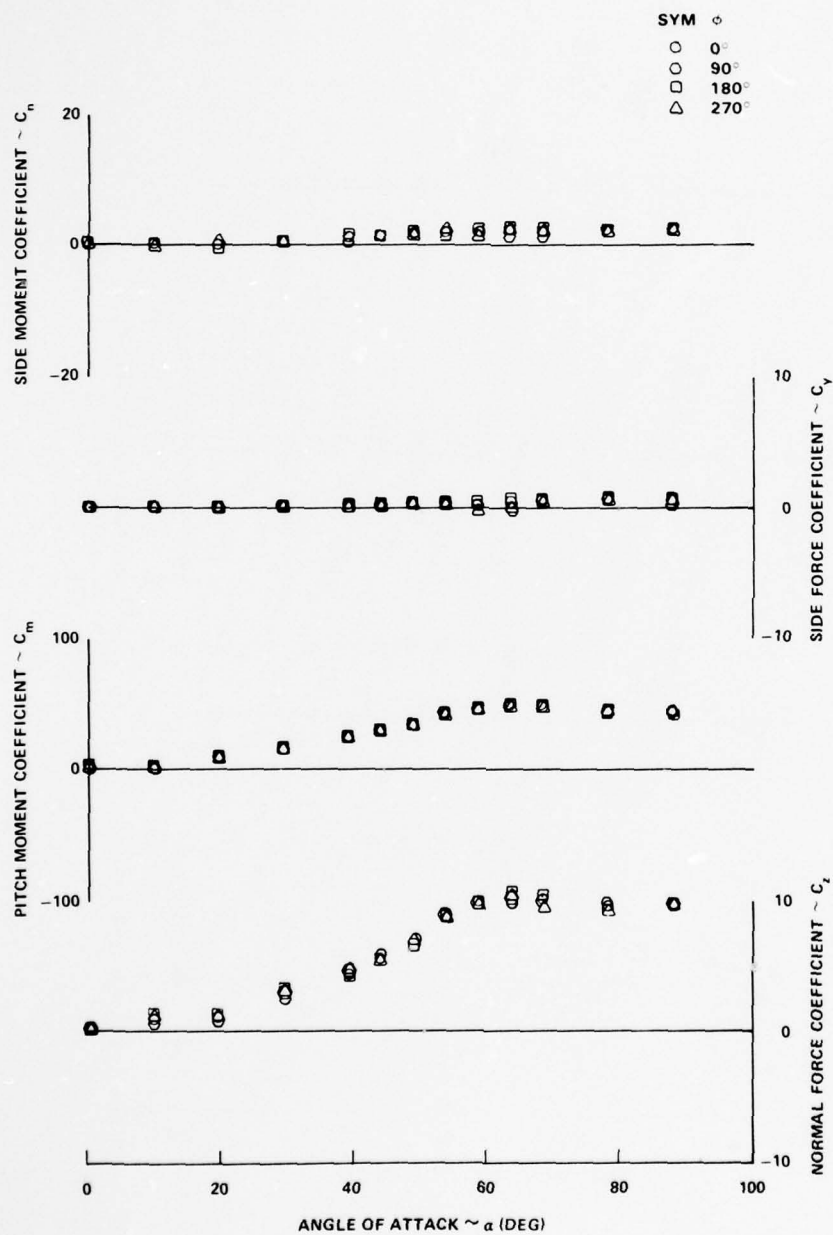with Blunted Nose (CVM)
V = 140 mph

Figure 17. Aerodynamic Characteristics of Blunted Ogive
Cylinder with Gap (CVM)
V = 85 mph

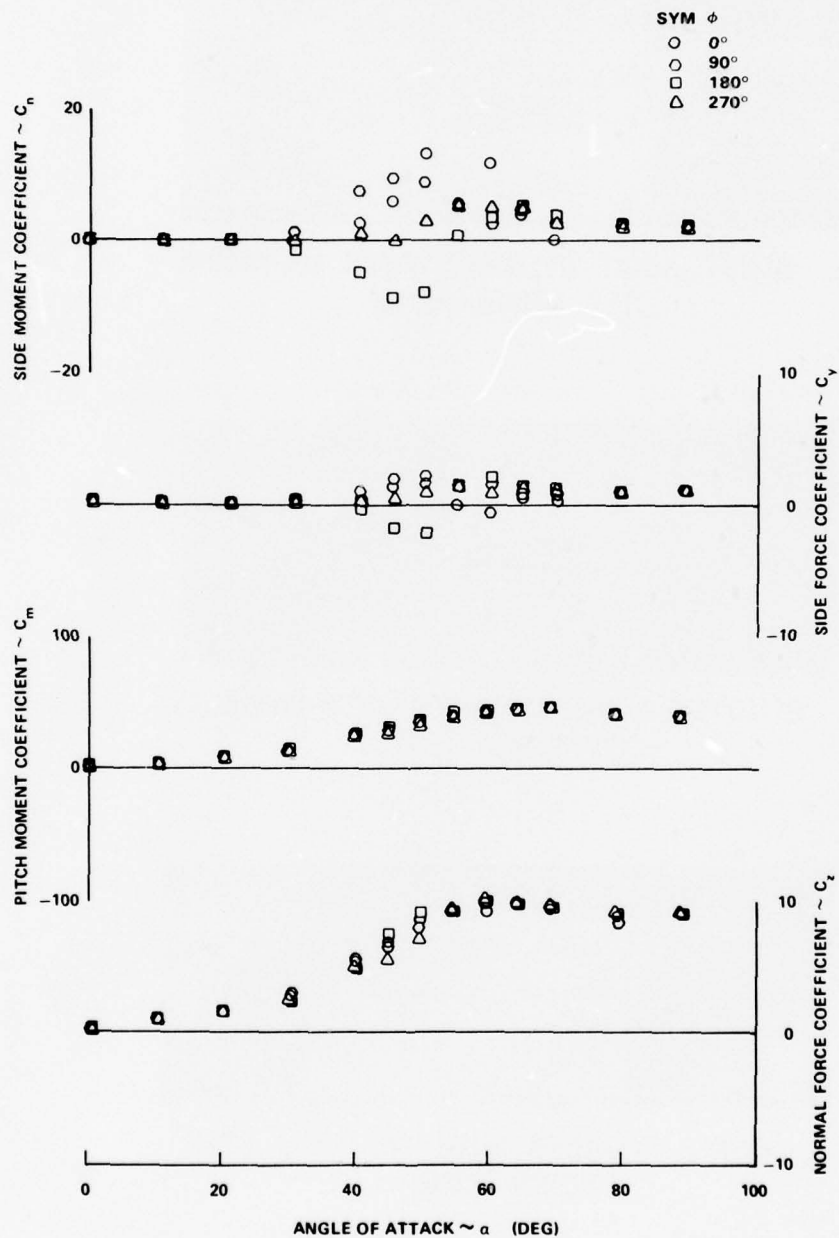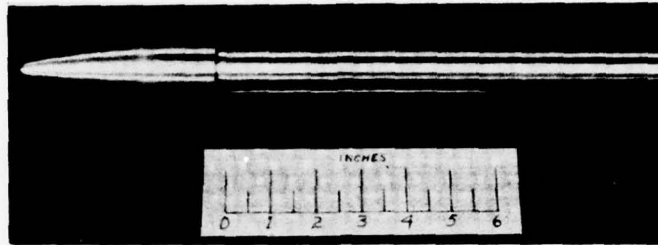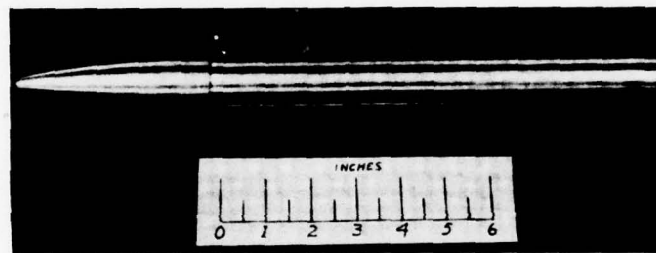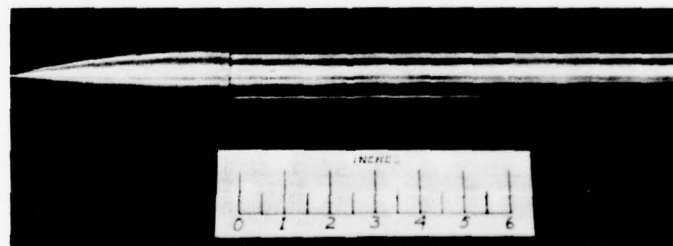22

Figure 18.   Aerodynamic Characteristics of Blunted Ogive
Cylinder with Gap (CVM)
V = 120 mph

23

a. BLUNT OGIVE CYLINDER WITH MAXIMUM
STEP DOWN (CVM)

b. BLUNTED OGIVE CYLINDER WITH MINIMUM
STEP DOWN (CVM)

c. OGIVE CYLINDER WITH MINIMUM STEP
DOWN (CVM)

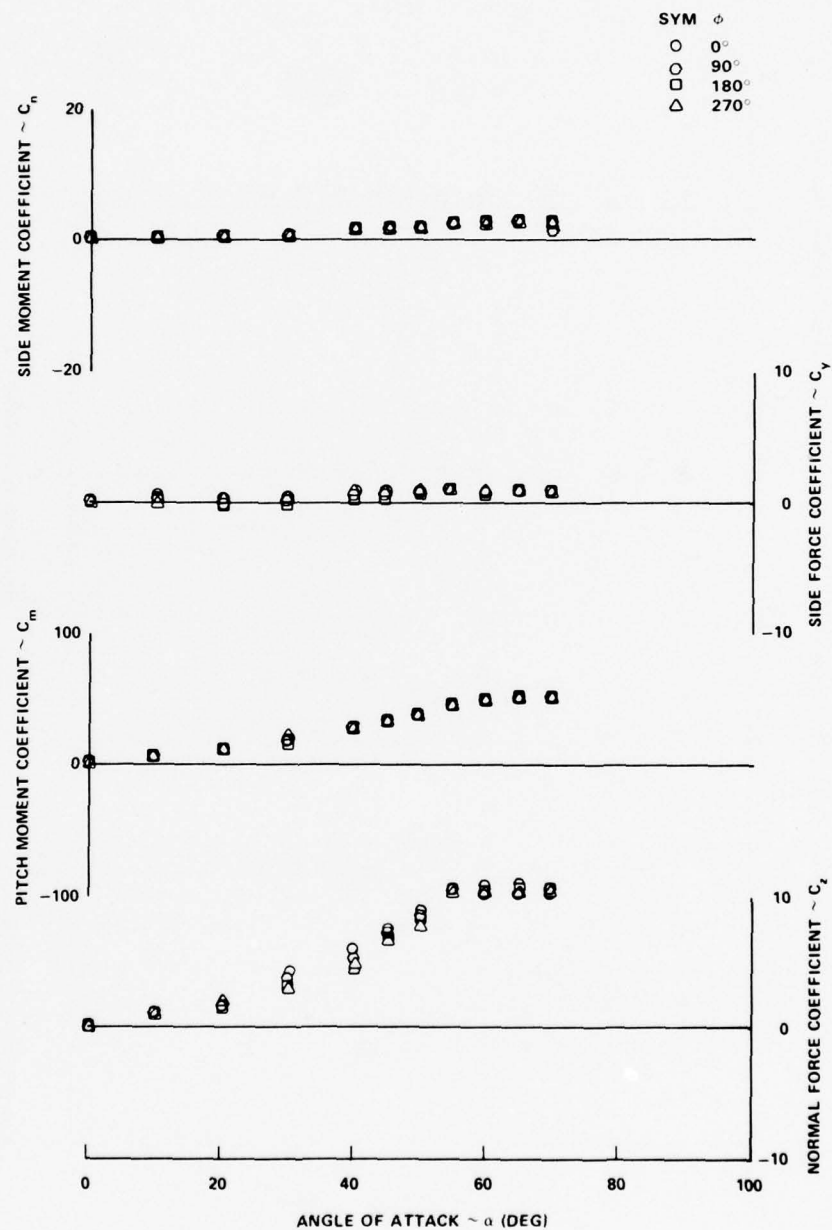Figure 19.   Ogive Cylinder Configurations with
Step Downs

24

Figure 20. Aerodynamic Characteristics of Blunted Ogive
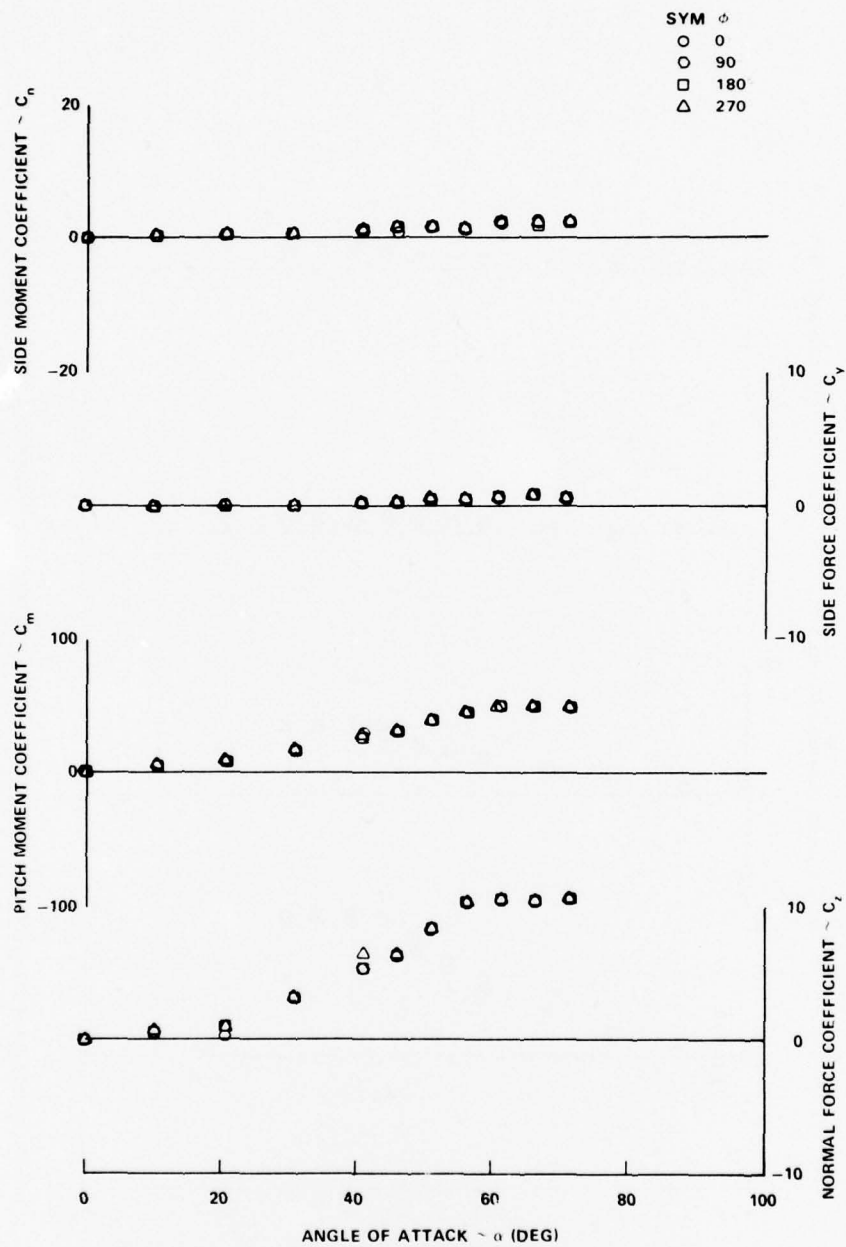Cylinder with Minimum Step Down (CVM)
V = 85 mph

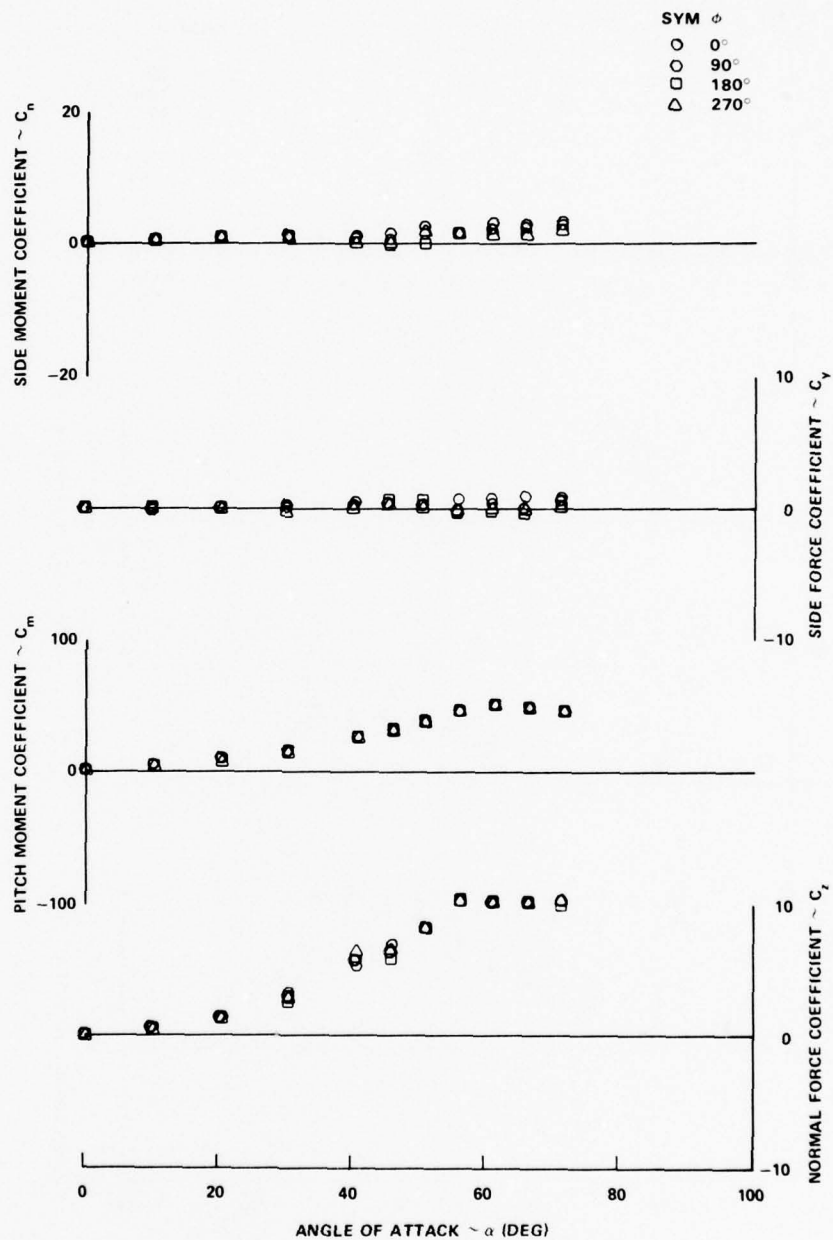Figure 21. Blunted Ogive Cylinder with Minimum Step Down
(CVM) V = 120 mph

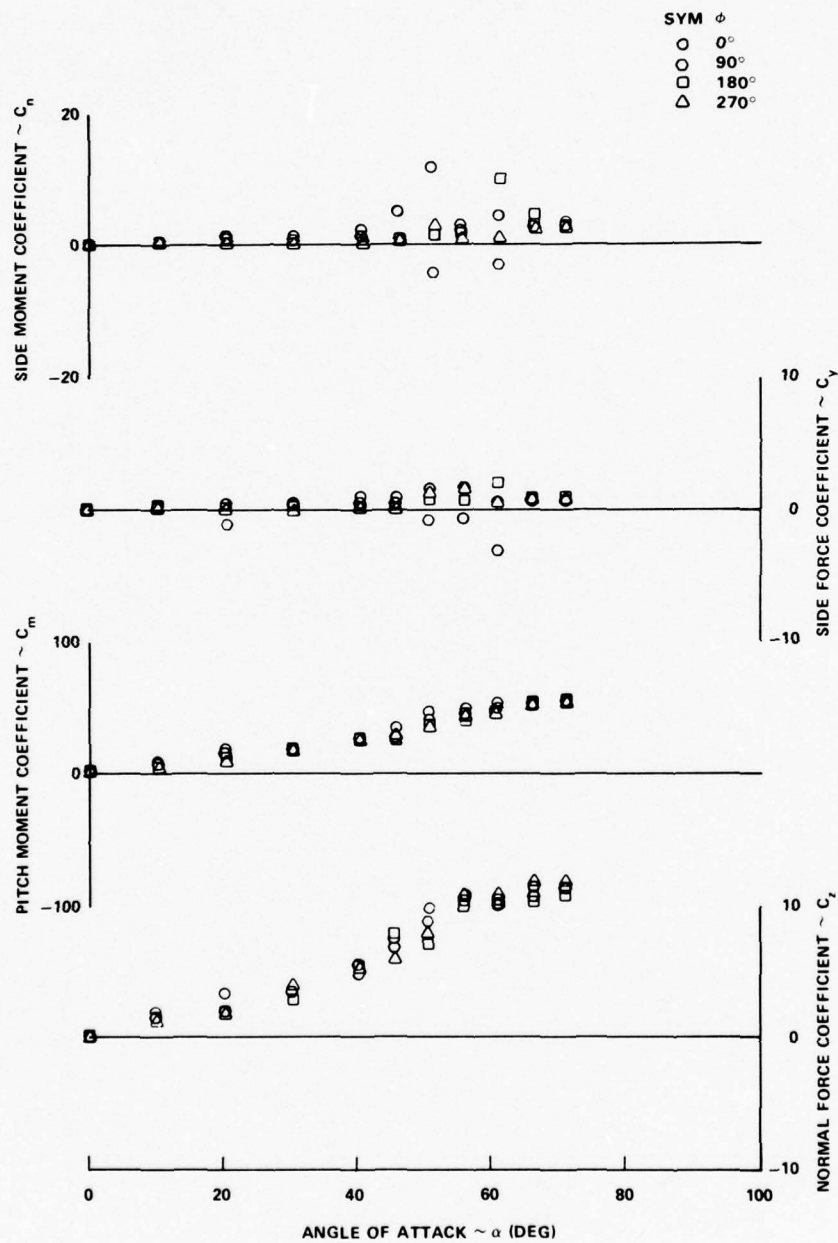Figure 22. Blunted Ogive Cylinder with Minimum Step Down
(CVM) V = 140 mph

Figure 23. Aerodynamic Characteristics of Pointed Ogive
Cylinder with Minimum Step Down
(CVM) V = 85 mph

Figure 24.   Aerodynamic Characteristics of Pointed Ogive
Cylinder with Minimum Step Down (CVM)
V = 120 mph

Figure 25.   Aerodynamic Characteristics of Pointed Ogive
Cylinder with Minimum Step Down (CVM)
V = 140 mph

**a. PARABOLIC NOSE CYLINDER
BODY (CVM)**
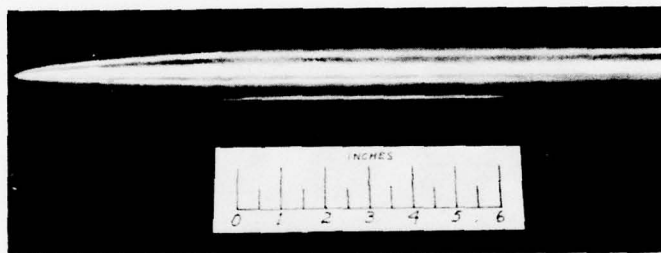
**b. PARABOLIC NOSE CYLINDER
BODY WITH MINIMUM STEP DOWN
(CVM)**

Figure 26.   Parabolic Nose Cylinder Models
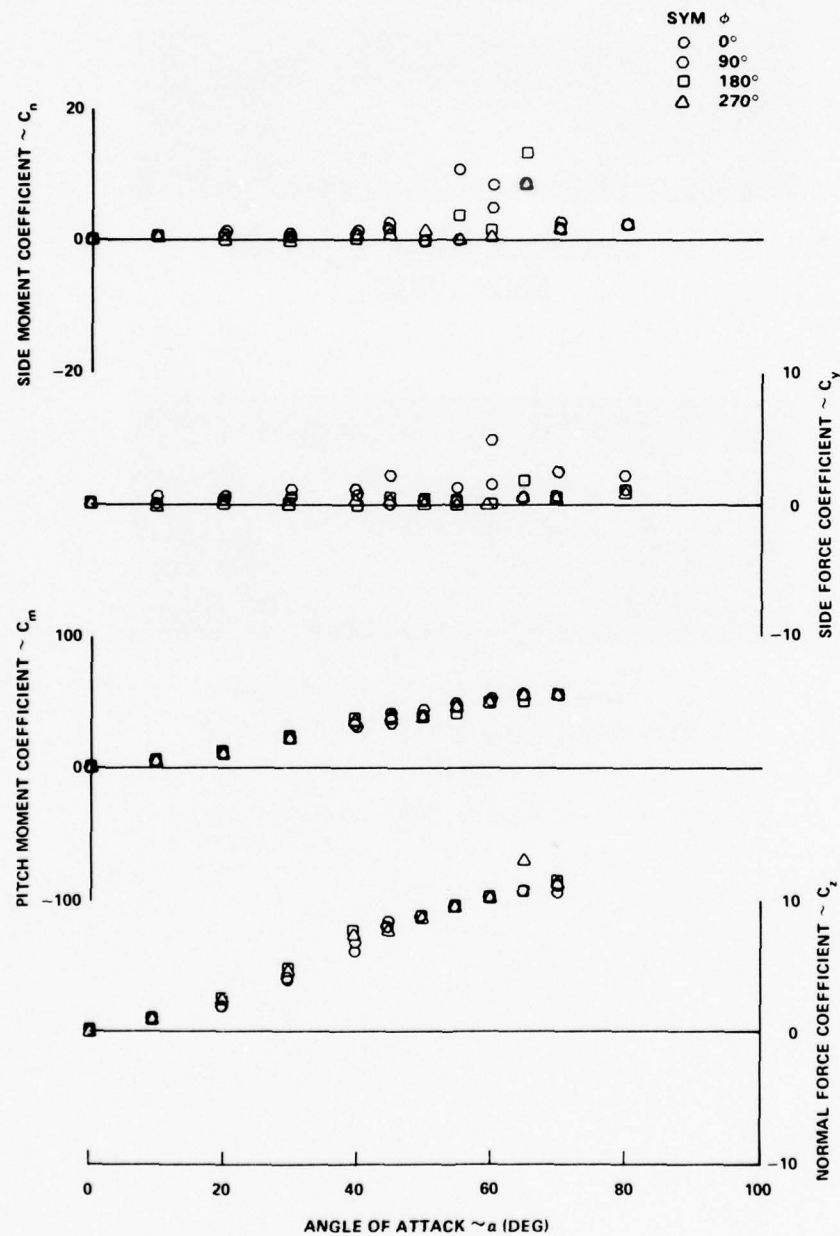
Figure 27. Aerodynamic Characteristics of Parabolic Nose
Cylinder V = 85 mph

32
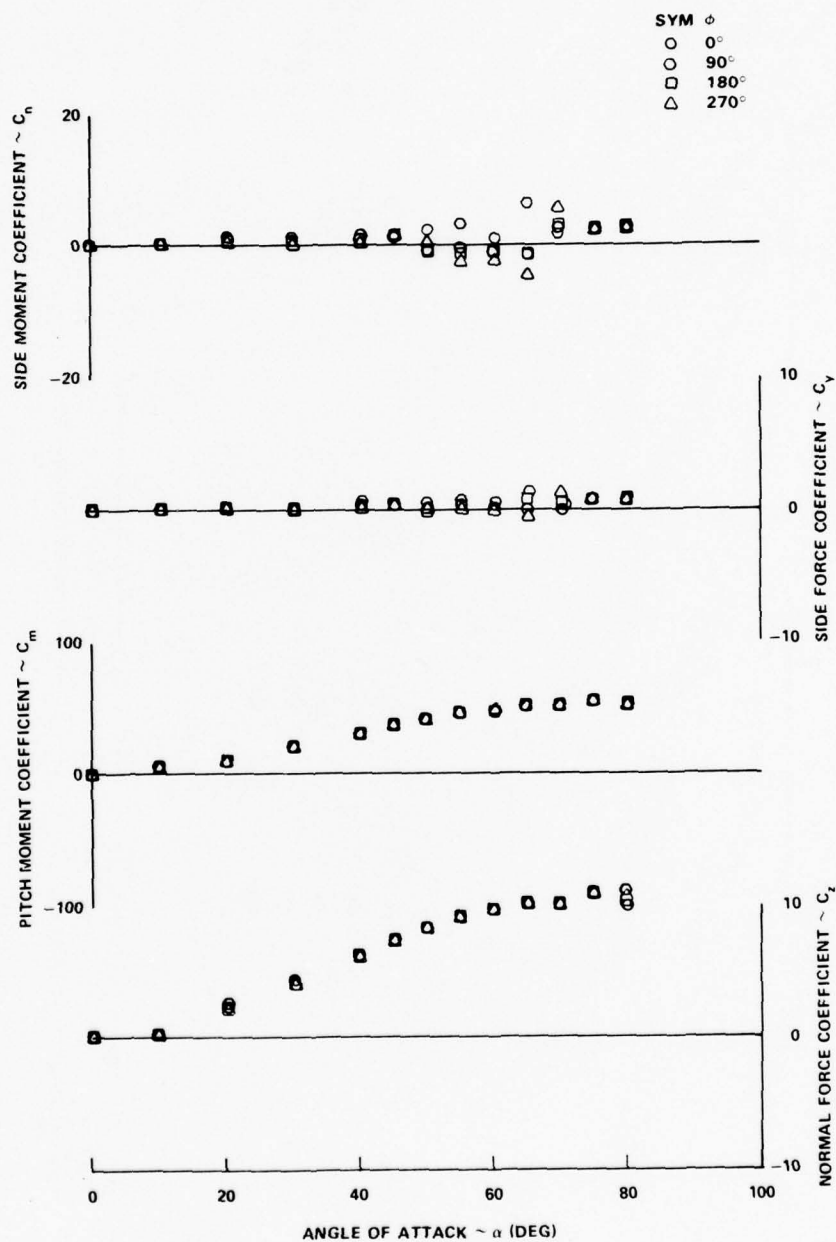
Figure 28.   Aerodynamic Characteristics of Parabolic Nose
Cylinder (CVM) V = 120 mph

33
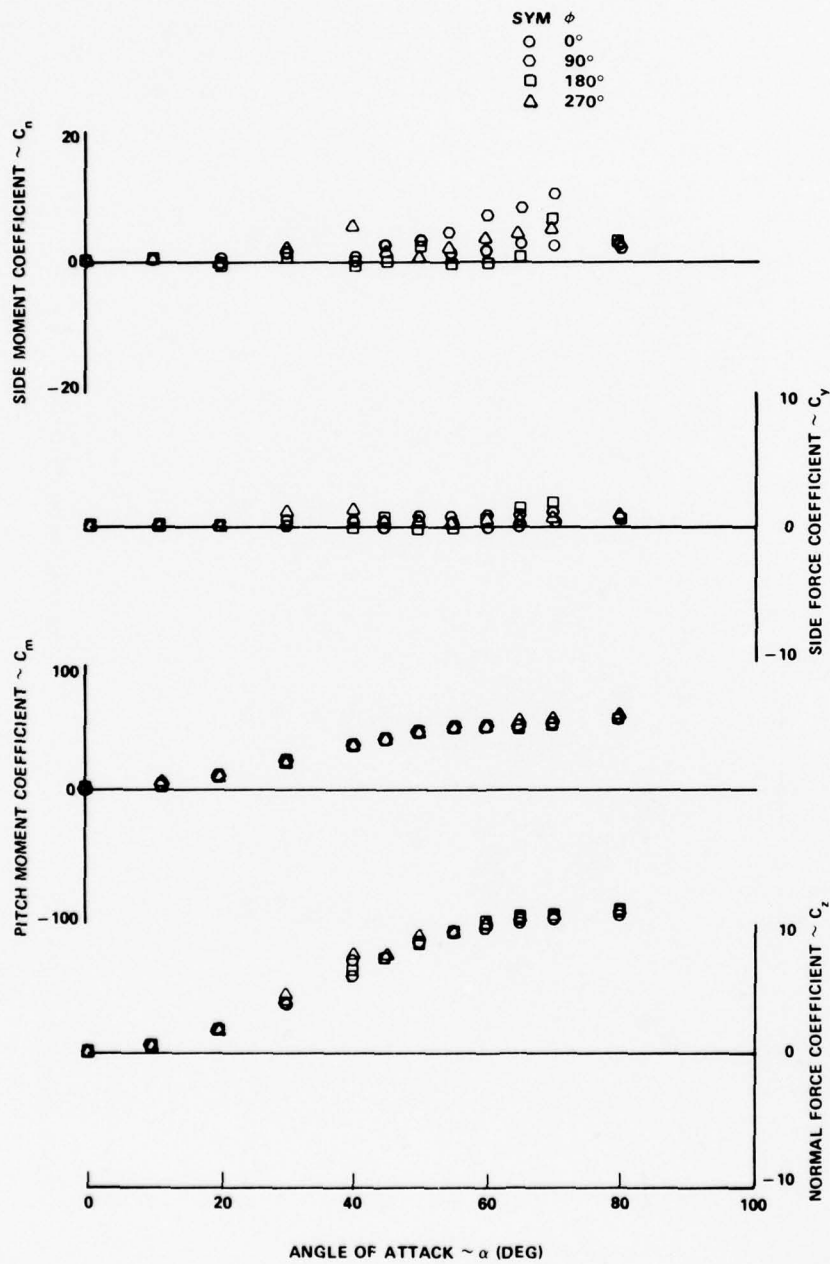
Figure 29. Aerodynamic Characteristics of Parabolic Nose
Cylinder (CVM) V = 140 mph

34
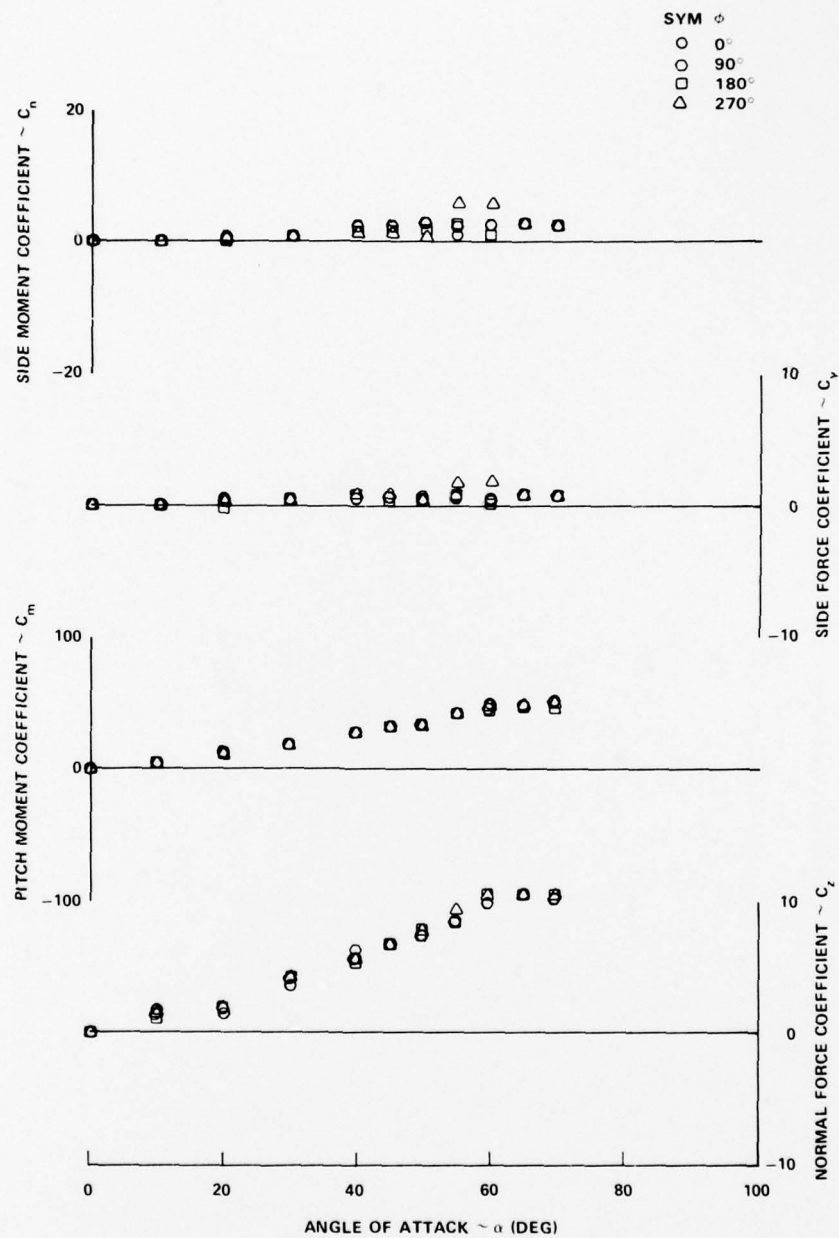
Figure 30. Aerodynamic Characteristics of Parabolic Nose
Cylinder with Minimum Step Down (CVM)
V = 85 mph
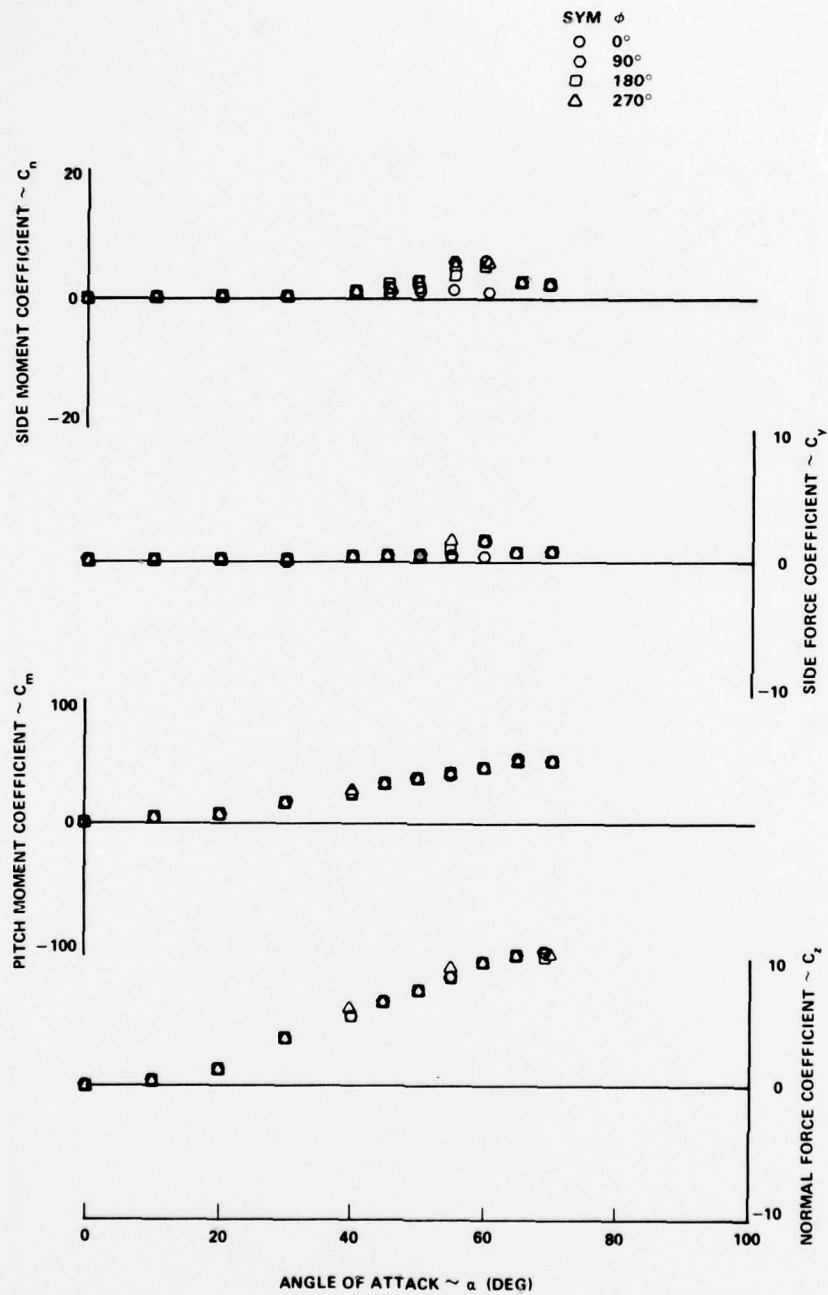
Figure 31.   Aerodynamic Characteristics of Parabolic Nose
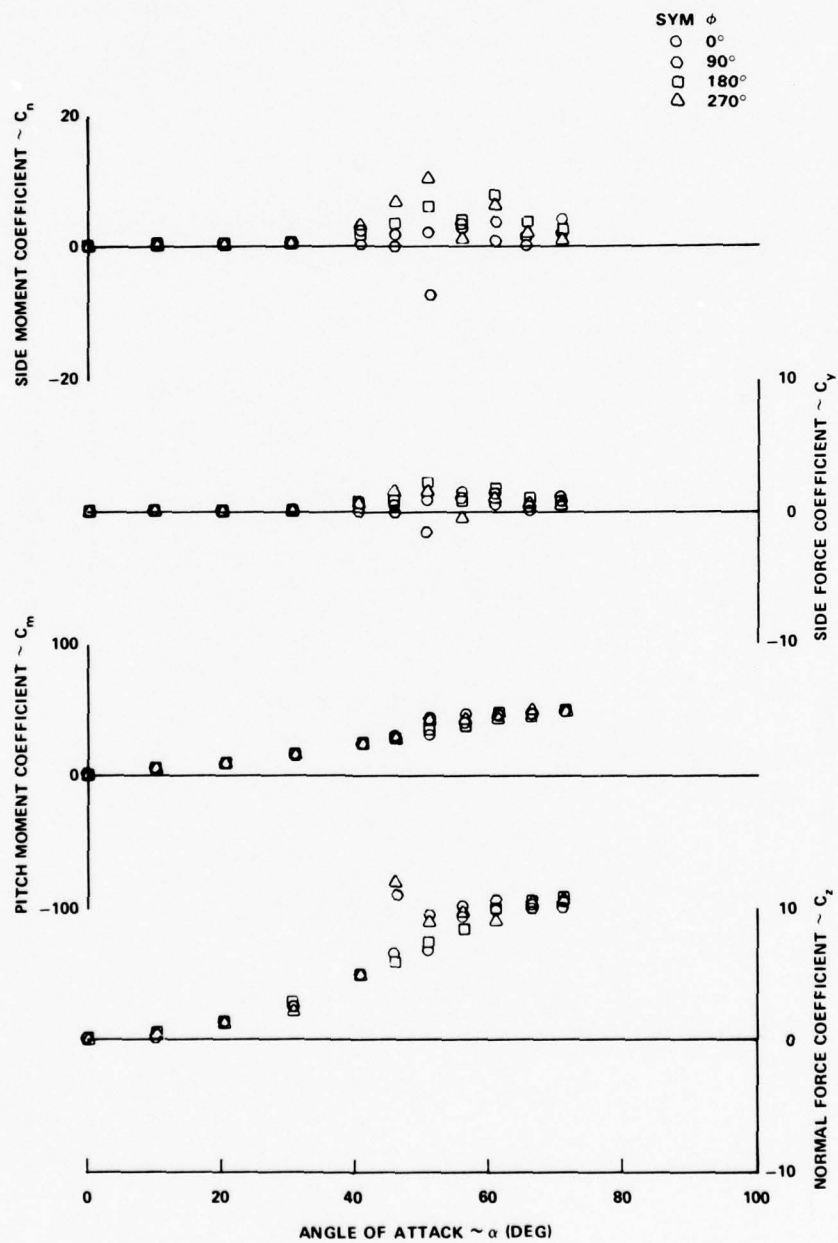Cylinder with Minimum Step Down
V = 120 mph

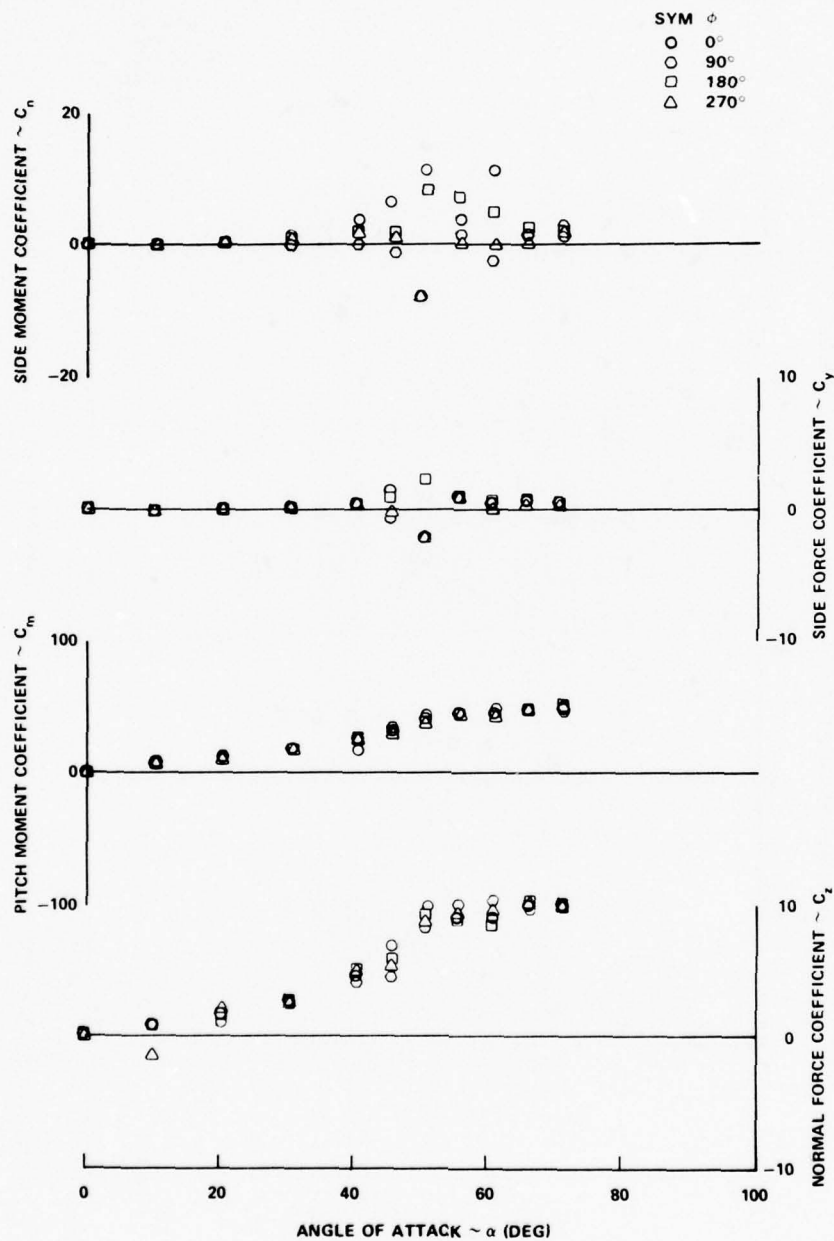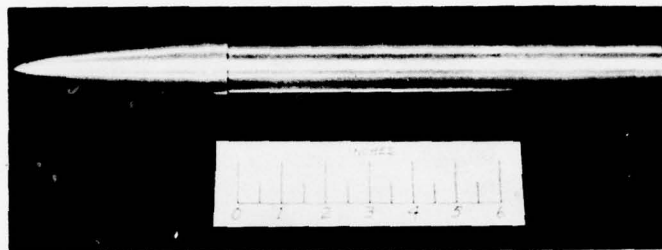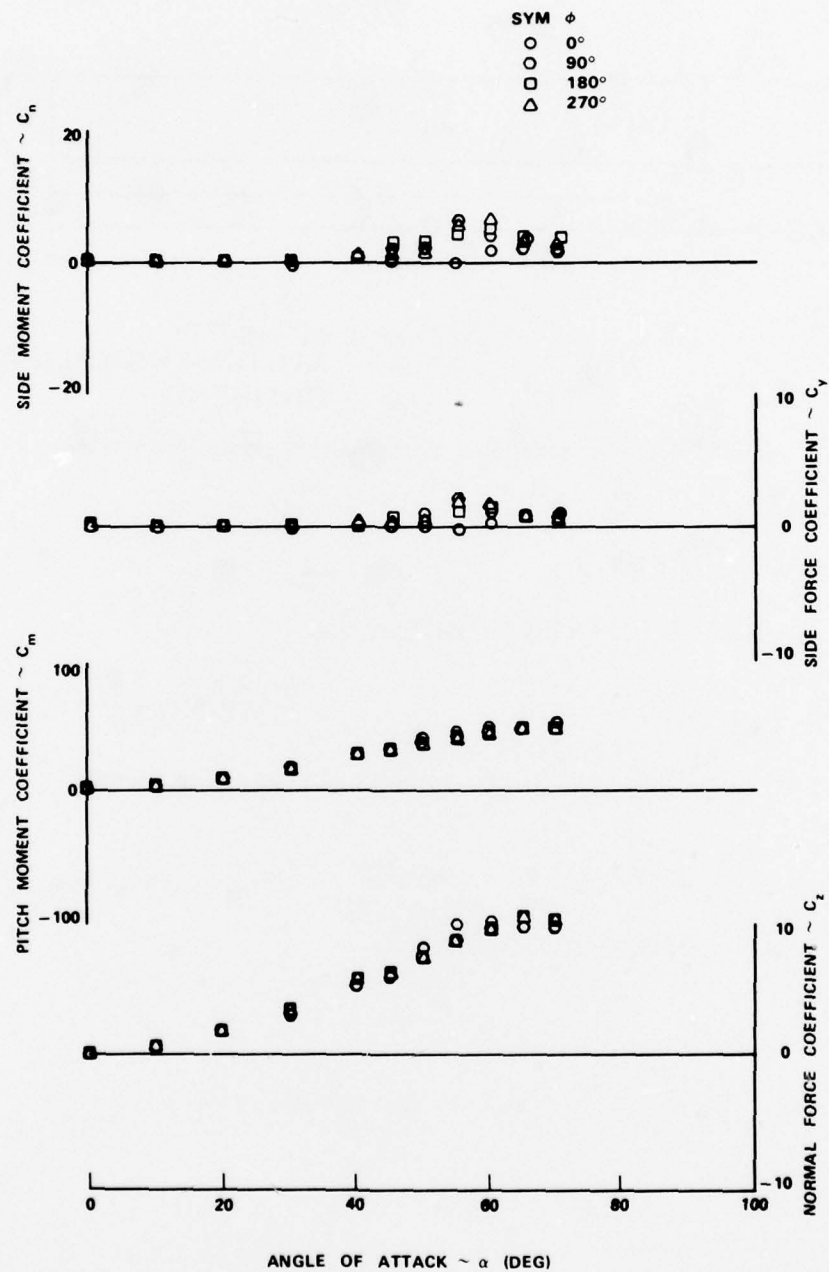Figure 32. Aerodynamic Characteristics of Parabolic Nose
Cylinder with Minimum Step Down
V = 140 mph

37

0.173R
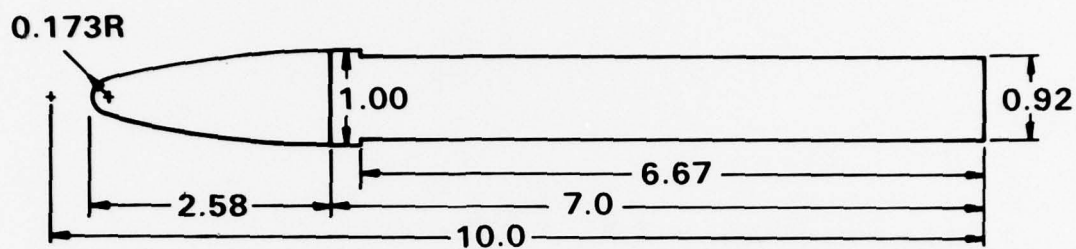
Figure 33. Ogive Cylinder Modified for Near Minimum Side Moment

ALL DIMENSIONS IN CALIBERS

1.00

0.92

6.67

2.58

7.0

10.0

SMOKE RAKE

ANTI-TURBULENCE SCREENS

WORKING SECTIONS

MODEL

SUPPORT

REDUCTION CONE

CAMERA
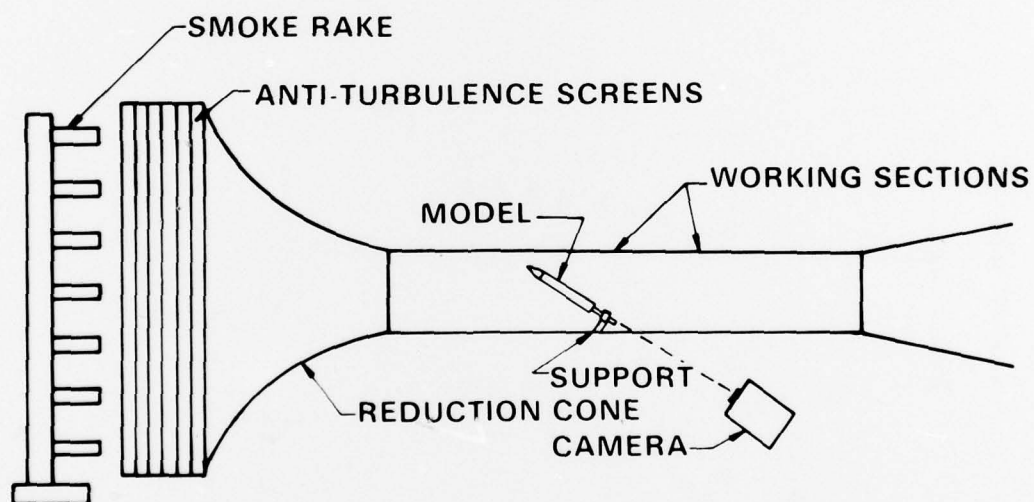
Figure 34. Sketch of Wind Tunnel and Model[8] (Side View)

38
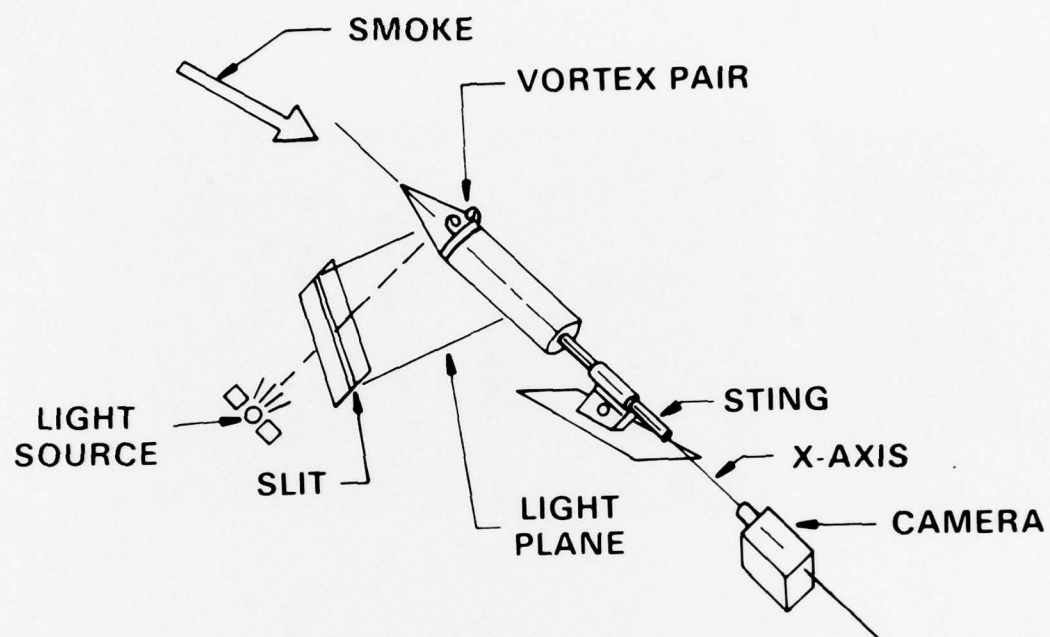
Figure 35. Sketch of Experimental Setup for Obtaining Smoke Pictures[8]

NOSE STATION

MID STATION

AFT STATION

POINTED OGIVE CYLINDER

BLUNTED OGIVE CYLINDER WITH
MINIMUM STEP DOWN
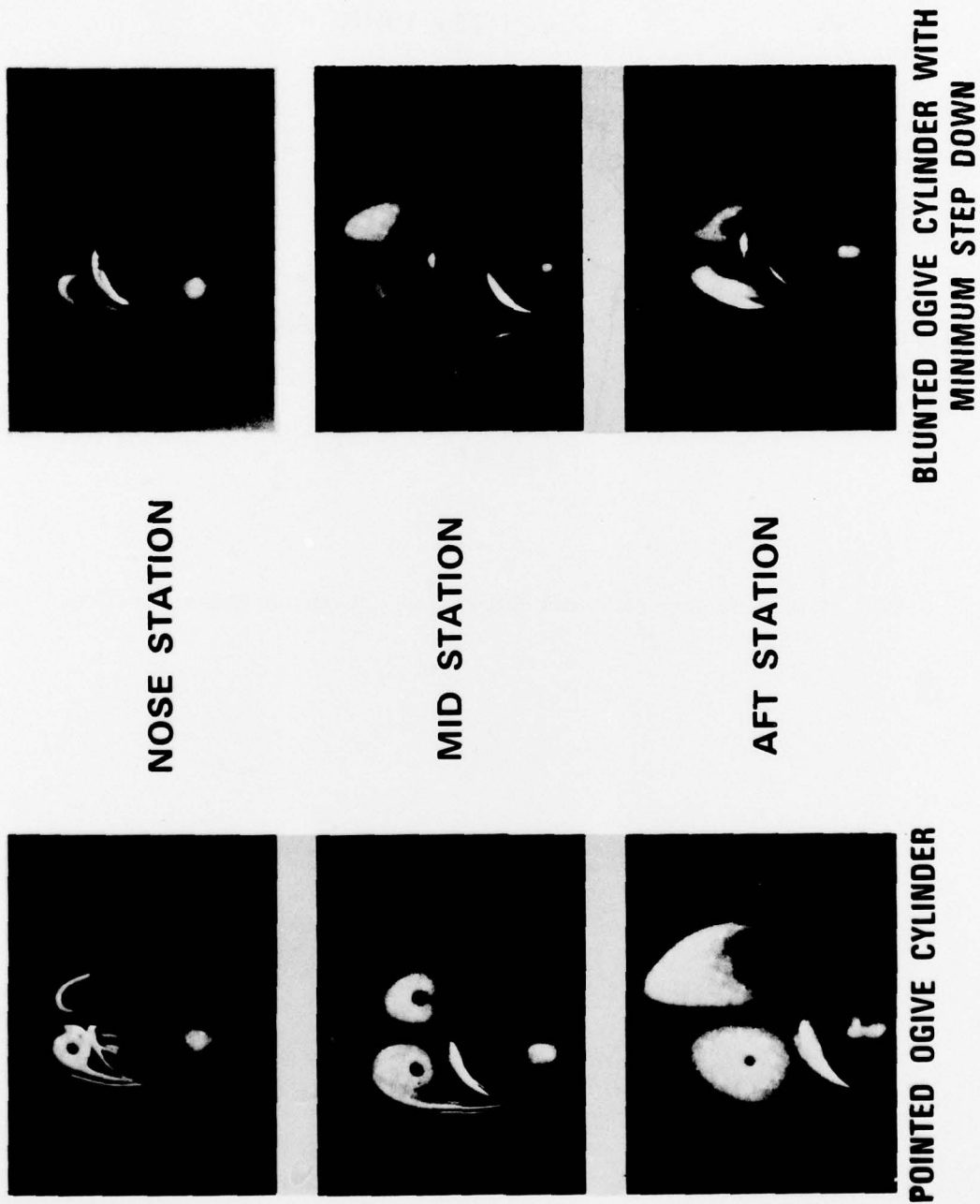
Figure 36. Flow Visualization of the Leeward Wake Structure of Ogive Cylinder Models
V = 30 ft/sec α = 35°

NOSE STATION

MID STATION

AFT STATION

POINTED OGIVE
CYLINDER

BLUNTED OGIVE CYLINDER WITH
MINIMUM STEP DOWN

Figure 37. Flow Visualization of the Leeward Wake Structure of Ogive Cylinder Models
$V = 30$ ft/sec $\alpha = 45°$

41

REFERENCES

1. Anshal I. Neihouse, Walter J. Kilman, and Stanley H. Scher, *Status of Spin Research for Recent Airplane Designs*, NASA TR-R-57, 1960.

2. Joseph R. Chambers, Ernie L. Anglin, and James S. Bowman, Jr., *Effects of a Pointed Nose on Spin Characteristics of a Fighter Airplane Model Including Correlation With Theoretical Calculations*, NASA TN D-5921, 1970.

3. Andrew B. Wardlaw, Jr., and Alfred M. Morrison, *Induced Side Forces on Bodies of Revolution at High Angle-of-Attack*, Naval Surface Weapons Center, White Oak Laboratory Technical Report NSWC/WOL/TR 75-176, Silver Spring, MD, 1 November 1975.

4. Paul L. Coe, Jr., Joseph R. Chambers, and William Litko, *Asymmetric Lateral - Directional Characteristics of Pointed Bodies of Revolution at High Angles-of-Attack*, NASA TN-D-7095, November 1972.

5. W. H. Clark, J. R. Peoples, and M. M. Briggs, *Occurrence and Inhibition of Large Yawing Moments During High-Incidence Flight of Slender Missile Configuration*, Journal of Spacecraft and Rockets, Vol. 10, No. 8, August 1973.

6. L. H. Jorgensen, *Prediction of Static Aerodynamic Characteristics for Slender Bodies Alone and with Lifting Surfaces to Very High Angles-of-Attack*, NASA Technical Report NASA TR-474, Ames Research Center, Moffett Field, CA, September 1977.

7. A. Flatau, "Facilities and Capabilities of Aerodynamic Group Research Laboratories," Edgewood Arsenal, Edgewood, MD, EASP 100-70, June 1970.

8. Robert C. Nelson, "Flow Visualization Study of the Leeward Wake Structure Around Several Slender Wind Tunnel Models," University of Notre Dame, South Bend, IN, Purchase Order N60921-78-M-B424.

DISTRIBUTION

Superintendent
U. S. Naval Academy
Annapolis, MD 21402
ATTN: Head, Aerospace Department
       Technical Library   (2)

Superintendent
U. S. Naval Postgraduate School
Monterey, CA 95076
ATTN: Head, Mechanical Engineering Department
       Head, Department of Aeronautics
       Technical Library   (2)

Commanding Officer
Naval Ordnance Station
Indian Head, MD 20640
ATTN: Code 525A1, Mr. David Krause
       Technical Library   (2)

Systems Research Laboratory, Inc.
2800 Indian Ripple Road
Dayton, OH 45440
ATTN: Dr. Charles W. Ingram
       Technical Library

Commander
Naval Air Systems Command
Washington, DC 20360
ATTN: AIR-320, Mr. Bill Volz
       Technical Library   (2)

Commander
Naval Sea Systems Command
Washington, DC 20360
ATTN: SEA-03, Mr. Lionel Pasiuk
       Technical Library   (2)

Commander
Naval Material Command
Washington, DC 20360
ATTN: Technical Library   (2)

Commander
Naval Weapons Center
China Lake, CA 93555
ATTN: Code 4063, Mr. Ray Van Aken
       Code 4063, Dr. Bill Clark
       Technical Library

Commander
Pacific Missile Test Center
Point Mugu, CA 93041
ATTN: Mr. Joe Rom
       Richard Larson
       James Saffell
       Technical Library   (2)

Commander
Ballistic Research Laboratory
Aberdeen Proving Ground, MD 21005
ATTN: Dr. C. H. Murphy
       Mr. L. McAllister
       Dr. A. Platou
       Mr. B. McCoy

Commander
Department of the Army
U.S. Army Armament Research and Development Command
Dover, NJ 07801
ATTN: Mr. A. Loeb

Commander
U. S. Army Missile Command
Redstone Arsenal, AL 35809
ATTN: Mr. Ray Deep (DRSMI)

Office of Chief of Research and Development
Washington, DC 20310
ATTN: Technical Library   (2)

Commander
Army Chemical Center
Edgewood, MD 21040
ATTN: Abraham Flatau
       Miles Miller
       Don Olson
       Joseph Huerta
       Technical Library   (2)

```
Commanding Officer
U. S. Air Force Armament Laboratory (AFATL)
Eglin Air Force Base, FL  32542
ATTN:  Dr. Daniel
       Mr. C. Butler
       Mr. C. Matthews
       Mr. K. Cobb
       Mr. E. Sears
       Mr. Gerald Winchenbach
       Technical Library                                    (2)


Superintendent
U. S. Air Force Academy
Colorado Springs, CO  80912
ATTN:  Technical Library                                    (2)


Commanding Officer
Air Force Flight Dynamics Laboratory
Wright-Patterson Air Force Base, OH  45433
ATTN:  Mr. E. Flinn (FCG)
       Dr. G. Kurylowich (FGC)
       Technical Library                                    (2)


Applied Physics Laboratory
The Johns Hopkins University
8621 Georgia Avenue
Silver Spring, MD  20910
ATTN:  Dr. L. L. Cronvich
       Mr. Edward T. Marley
       Dr. Gordon Dugger
       Technical Library                                    (2)


Director
Advanced Research Projects Agency
Department of Defense
Washington, DC  20305
ATTN:  Technical Library                                    (2)


Director
Defense Research Engineering
Department of Defense
Washington, DC  20305
ATTN:  Technical Library                                    (2)


Commander
George C. Marshal Flight Center
Huntsville, AL  35804
ATTN:  Technical Library                                    (2)
```

Commander
Harry Diamond Laboratories
Washington, DC 20013
ATTN: Technical Library   (2)

Commanding Officer
USAF Office of Scientific Research
Washington, DC 20330
ATTN: Technical Library   (2)

Commanding Officer
Arnold Engineering Development Center
USAF
Tullahoma, TN 37389
ATTN: Mr. J. Uselton
      Mr. L. M. Jenke
      Mr. W. B. Baker, Jr.
      Technical Library   (2)

Headquarters, USAF
Systems Command
Andrews Air Force Base, MD 20331
ATTN: CAPT William Miklos
      Technical Library   (2)

Headquarters, USAF
Washington, DC 20330
ATTN: Technical Library   (2)

Commanding Officer
Flight Research Center
Edwards Air Force Base, CA 93523
ATTN: Technical Library   (2)

Commanding Officer
Air Force Rocket Propulsion Laboratory (AFSC)
Department of the Air Force
Edwards, CA 93523
ATTN: MAJOR Washburn
      Technical Library

Commanding Officer
U. S. Air Force Systems Command
Regional Offices
c/o Department of the Navy
Washington, DC 20360
ATTN: Technical Library   (2)

Director
Defense Research and Engineering
Department of Defense
Washington, DC 20301
ATTN: Technical Library

Raytheon Company
Spencer Laboratory
Burlington, MA 01803
ATTN: Mr. J. A. Greco
       Technical Library

Lockheed Missiles and Space Co., Inc.
Department 81-10, Bldg. 154
Sunnyvale, CA 94088
ATTN: Dr. Lars E. Erisson

Nielsen Engineering and Research, Inc.
510 Clyde Avenue
Mountain View, CA 94043
ATTN: Dr. Jack Nielson

California Polytechnic Institute
Aeronautical Engineering Department
San Luis Obispo, CA 93407
ATTN: Dr. John D. Nicolaides
       Technical Library

Defense Documentation Center
Cameron Station
Alexandria, VA 22314   (12)

Library of Congress
Washington, DC 20390
ATTN: Gift and Exchange Division   (4)

Local

E41
G44
K
K01
K20
K21
K81 (Mr. M. V. Krumins)
K82 (Mr. F. J. Regan)
X210   (2)
X2101